Risø-R-1268(EN)

Description of the Rødsand field measurement

Bernhard Lange, Rebecca Barthelmie, Jørgen Højstrup

Risø National Laboratory, Roskilde
May 2001

Abstract

The meteorological and oceanographic field measurement Rødsand has been established 1997 at the site of the planned offshore wind farm Rødsand, 12 km south of Lolland. Its primary aim is to provide data about the environmental conditions needed in the planning process of the wind farm. Additionally, the field measurement provided a valuable data set for scientific research. This report provides a documentation of the Rødsand field measurement, including the site, the measurement station itself, the extensive quality control of the data and the data processing.

ISBN 87-550-2885-3(Internet)
ISSN 0106-2840

Contents

1 Introduction

The offshore meteorological measurement mast Rødsand has been built about 12 km south of Lolland at the site of the proposed wind farm Rødsand. It has been running as a meteorological monitoring station since 1996. In 1998 a wave and current measurement was installed additionally to monitor waves, current and water level at the site. The meteorological measurement is ongoing although the wave and current instrumentation was removed in March 2001.

A large amount of high quality data have been collected at the Rødsand field measurement. They have been analysed in several projects, where (Højstrup et al., 1997), (Barthelmie et al., 1998) and (Barthelmie et al., 1999) focused mainly on the atmospheric data, while (Lange, 2000) was mainly concerned with the oceanographic data. The data and the analysis projects proved to be essential in planning the wind farm Rødsand. Furthermore, the field measurement also provided a very valuable data base for scientific research in the field of air-sea interaction.

Despite the large amount of work already done with the data comprehensive documentation of the field measurement Rødsand is incomplete. The present report aims to fill this gap. It is therefore obvious that the larger part of the information contained in this report has been collected from the earlier reports, especially from (Lange, 2000).

The report is organised in four parts. In the following two chapters the site of the measurement station and the instrumentation employed for the measurement are described. The instrumentation was modified and an additional data acquisition system was installed in 1999 in response to technical problems with the measurement station. Both data acquisition systems and the different mast layouts, which have been used over the time, are documented here.

The largest part of this report is devoted to the description of the extensive quality control. Quality control has been made first for the fast sampled data to search for instrument problems which might not be detectable in the processed statistical time series. This is described in chapter 4.1. The main problems found were noise in the wave and sonic measurements and data clipping in the wave and current measurements. Data filtering and screening procedures have been developed to detect and where possible correct the measurements.

In a second step quality control has been performed for the time series of the statistical data (see chapter 4.2). Instrument failures, direction calibrations and corrections for flow distortion due to the measurement mast were the subject here. For parameters calculated from the wave spectra, a criterion was established to test for the validity of the derivation.

Finally, in chapter 5 the data processing and the resulting data bases are documented. It has been distinguished between a meteorological data base and a met-ocean data base, which contains only records where both meteorological and oceanographic data are available. This is the case for about 25% of the total measurement time.

2 Site description

2.1 Location

A meteorological and oceanographic measurement station has been established at Rødsand in the Danish Baltic Sea about 12 km south of the coast of Lolland. The position of the measurement mast is (UTM 32) 677642 m E and 6047287 m N (geographical co-ordinates 11° 44.758'E 54° 32.445'N). The oceanographic (wave and current) measurements are situated about 100 m south-west of the mast. The location of the mast is shown in Figure 1.

Figure 1: Rødsand measurement site

2.2 Water depths

The mean water depth at the location of the station is 7.7 m. The water depths around the station are 6.4-8.2m as given in the sea chart (see Figure 2). The sea bed surrounding the station does not show a distinct slope. An area with shallower water can be seen north of the station.

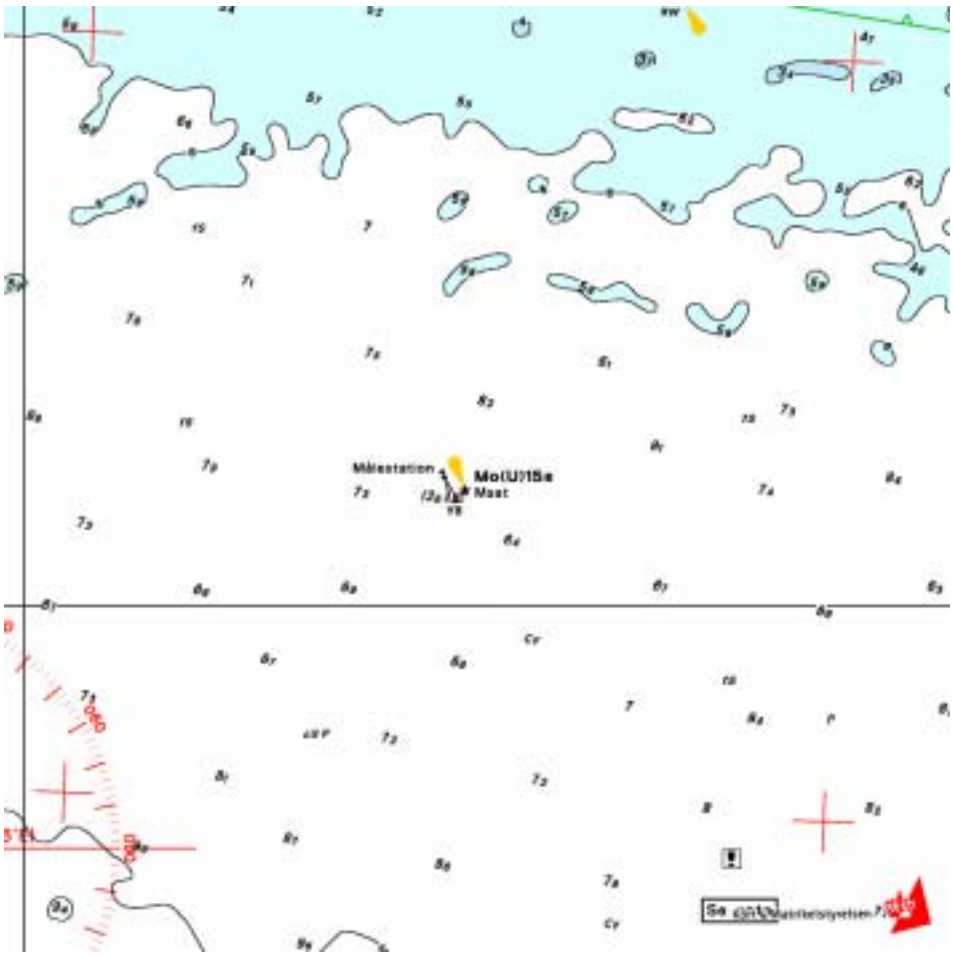

Figure 2: Sea chart of the near vicinity of the Rødsand measurement station (shown as 'Målestation' at the centre) (with kind permission from 'Kort & Matrikelstyrelsen, Denmark)

2.3 Fetch distances

The station Rødsand experiences a wide range of over water distances to the nearest land (fetch). The distance to the coast of Lolland and Falster is 12-18 km distance, Fehman is about 32-36 km away and the coast of Germany 43-84 km. In between there are narrow gaps to the west with about 110 km fetch and to the east with about 86 km fetch. Distances to the nearest land (fetch distances) versus direction are given in Table 1. The sand bank 'Rødsand' is located about 5 km north-east of the station. It is exposed at low water levels, but is submerged at high water levels.

Table 1: Fetch distances at Rødsand

direction [°] (geogr.)	fetch [km]	direction [°] (geogr.)	fetch [km]	direction [°] (geogr.)	fetch [km]
0	12	120	47	240	51
5	12	125	47	245	32
10	12	130	46	250	32
15	12	135	46	255	32
20	12	140	44	260	33
25	15	145	44	265	36
30	15	150	46	270	44
35	14	155	45	275	110
40	14	160	44	280	110
45	13	165	43	285	110
50	13 (6*)	170	44	290	16
55	13 (6*)	175	44	295	16
60	13 (6*)	180	43	300	18
65	12 (7*)	185	43	305	18
70	12 (7*)	190	48	310	17
75	13 (8*)	195	53	315	17
80	14	200	62	320	15
85	86	205	70	325	16
90	86	210	70	330	15
95	86	215	71	335	14
100	49	220	84	340	14
105	49	225	84	345	14
110	47	230	55	350	12
115	47	235	53	355	12

* sand bank above or below water depending on water level

2.4 Description of surrounding land areas

The station Rødsand is surrounded by the islands Lolland and Falster to the north, The island Fehman to the south-west and the mainland of Germany to the south (see Figure 1). All these land areas are very flat and no orographic effects on the air flow at Rødsand are expected. The land use of the areas is mainly agriculture, with scattered villages and some forests. A map of estimated roughness has been prepared from topographic maps of the areas. It is shown in Figure 3.

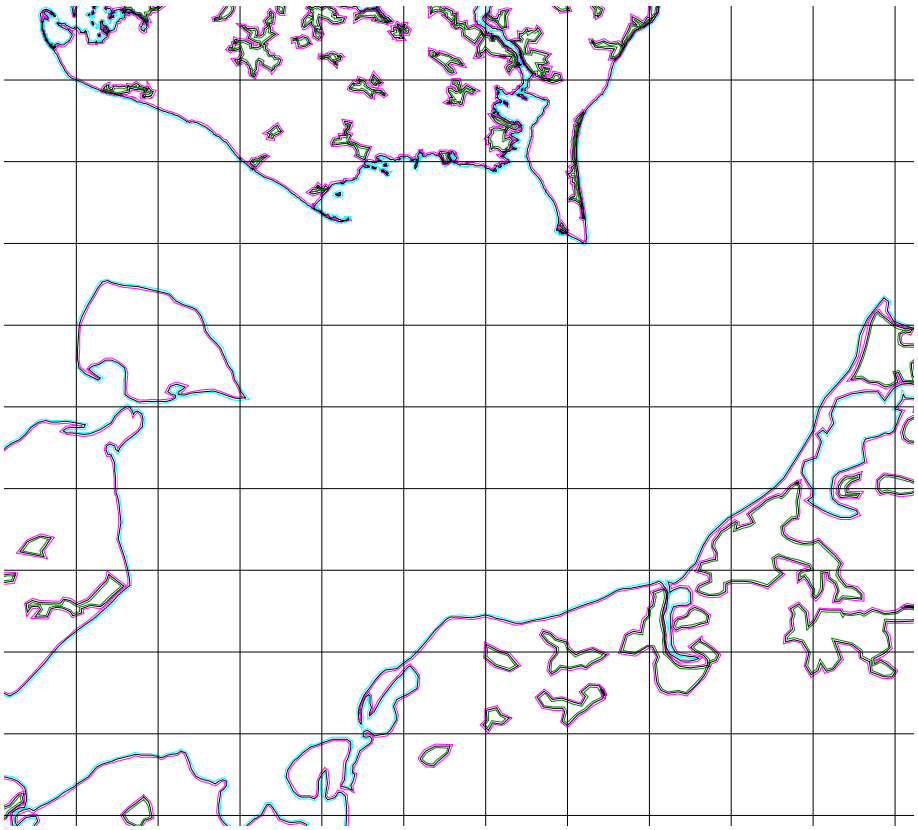

Figure 3: Map of roughness changes of the land areas surrounding the measurement station Rødsand; three terrain types have been distinguished: water (z_0=0.0002m), agricultural areas (z_0=0.1m) and forests or villages (z_0=0.4m)

3 Instrumentation

3.1 Station history

A 50 m high meteorological measurement mast was established at Rødsand in October 1996. In April 1998 an acoustic sea bed mounted wave gauge and a water current sensor were installed for oceanographic measurements. Since then simultaneous wind and wave measurements have been performed.
The availability of the station was unexpectedly low, mainly due to technical problems with the autonomous power supply and data transfer. Therefore in May 1999 a major change in the instrumentation of the meteorological mast was performed with the installation of an additional measurement system.
An analysis of the wave data revealed problems with the instrument. In response the acoustic wave recorder was upgraded and re-installed in October/November 1999. The wave and current instrumentation was removed in March 2001. The meteorological measurement is ongoing.

Figure 4: The meteorological mast of the Rødsand field measurement

3.2 Data acquisition systems

3.2.1 DAQ system

The original system was designed to operate meteorological instruments together with a sonic anemometer, a wave height sensor and an instrument to measure current speed and direction. The data acquisition (DAQ) system is capable of collecting and storing time series from fast response instruments including the sonic anemometer. The positions of the instruments installed in 1996 are shown in Figure 5. The data acquisition system stores half-hourly statistics (mean, maximum, minimum and standard deviations) for all variables. Additionally, the raw data time series are stored. The half-hourly statistical data are retrieved by remote communication via mobile phone. The raw time series are stored on two flash disks and are collected at site visits.

For the time stamp saved with the measurements DNT (Danish standard time) is used. The time stamp gives the time of the beginning of a measurement (averaging) period.

Due to problems with the power supply and communications, data availability was lower than expected and in 1999 a new system (the Aanderaa system) was

installed additionally. Both systems were operated in parallel until March 2001. In this re-instrumentation some instruments of the DAQ system were removed or remounted at different heights. The instrumentation currently operated and logged through the DAQ system after 5/99 is shown in Figure 7.

3.2.2 Aanderaa system

Aanderaa recorders are low-power systems designed to operate in harsh conditions and have a proven track record of reliability. Two recent innovations made the systems ideal for operation offshore:

1. The ability to collect the data via a satellite link enabling on-line system checking. This is essential if instrument problems are to be remedied in a timely fashion.
2. The design of a new wind speed processor (P2706a) which calculates standard deviations, gust and lulls (Hansen, personal communication, 1999).

Since each recorder has 11 channels available two data loggers are operated to provide sufficient channels. Figure 8 shows the instrumentation connected to the data loggers (marked as DL1 and DL2). Instrumentation has been distributed between the two loggers such that in the unlikely event of failure of a data logger basic meteorological data will still be available from the remaining logger. The satellite transmitter transmits data from data logger 1 (DL1) which is shown on a web site almost every hour. These data are checked daily to ensure all instruments are operating. Aanderaa recorders store 10 minute average data. Data are collected from the mast every 8-10 weeks when any routine maintenance is also conducted.

For the time stamp saved with the measurements GMT (Greenwich time) is used. The time stamp gives the time of the end of a measurement (averaging) period. GMT is one hour behind the DNT, which is used in the DAQ system.

3.3 Mast set-up

3.3.1 DAQ-system prior 5/99

Table 2 and Figure 5 show the instrumentation of the measurement mast prior to the changes in 5/99. Wave and current data are only collected since 4/98.

Boom orientations are 265º (SW) and 085º (NE) for all set-ups.

Table 2: Instrumentation of the Rødsand measurement prior to 5/99 (original instrumentation)

measured quantity	height above mean sea level of 7.7 m	instrument	boom	sampling rate
Wind speed	50.3 m	cup anemometer	SW	5 Hz
	29.8 m	cup anemometer	SW	5 Hz
	10.2 m	cup anemometer	SW	5 Hz
Wind direction	29.8 m	wind vane	NE	5 Hz
3 axis wind speed and temperature	46.6 m	Gill ultrasonic anemometer F2360a	SW	20 Hz
air temperature	10.0 m	Pt 100	NE	30 min mean
Temperature difference	49.8 m – 10.0 m	Pt 500	NE	30 min mean
Sea temperature		Pt 100	-	30 min mean
Sea level	-4.0 m	DHI AWR201 acoustic wave recorder	-	8 Hz
Sea current	-2.4 m	GMI current meter	-	8 Hz

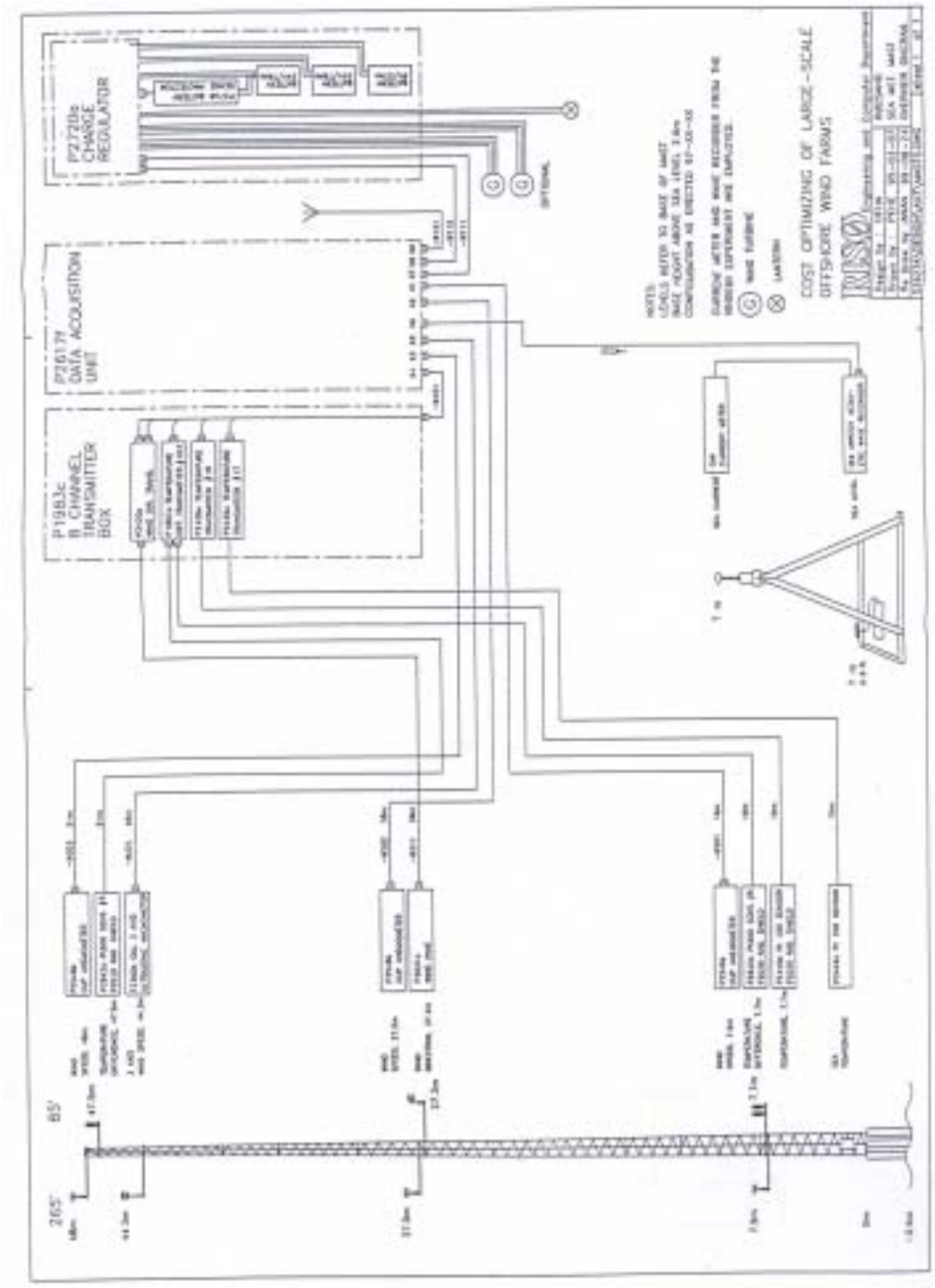

Figure 5: Set-up of the Rødsand mast with the DAQ-system prior to 5/99

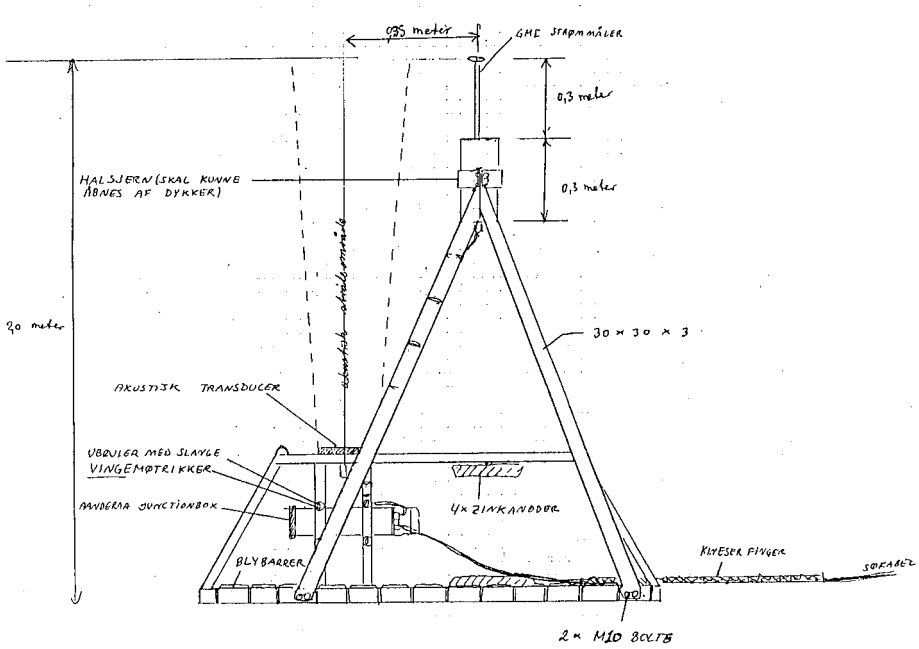

Figure 6: Sketch of the instrument set-up for the oceanographic measurement

3.3.2 DAQ-system after 5/99

The instrumentation has been changed in May 1999 with the additional installation of a new low power measurement system. With the mounting of the new system the old instruments were moved to different heights on new booms and additional instruments were mounted mainly on the old booms at the location of the old instruments. Table 2 and Figure 7 show the instrumentation of the measurement mast logged by the DAQ system after the changes in 5/99.

Table 3: Instrumentation of the Rødsand measurement logged by the DAQ system after 5/99

measured quantity	height above mean sea level of 7.7 m	instrument	boom	sampling rate
Wind speed	24.7 m	cup anemometer	SW	5 Hz
	7.4 m	cup anemometer	SW	5 Hz
Wind direction	24.9 m	wind vane	NE	5 Hz
3 axis wind speed and temperature	42.3 m	ultrasonic anemometer	SW	20 Hz
air temperature	10.0 m	Pt 100	NE	30 min mean
Temperature difference	49.8 m – 10.0 m	Pt 500	NE	30 min mean
Sea temperature		Pt 100	-	30 min mean
Sea level	-4.0 m	DHI AWR201 acoustic wave recorder	-	8 Hz
Sea current	-2.4 m	GMI current meter	-	8 Hz

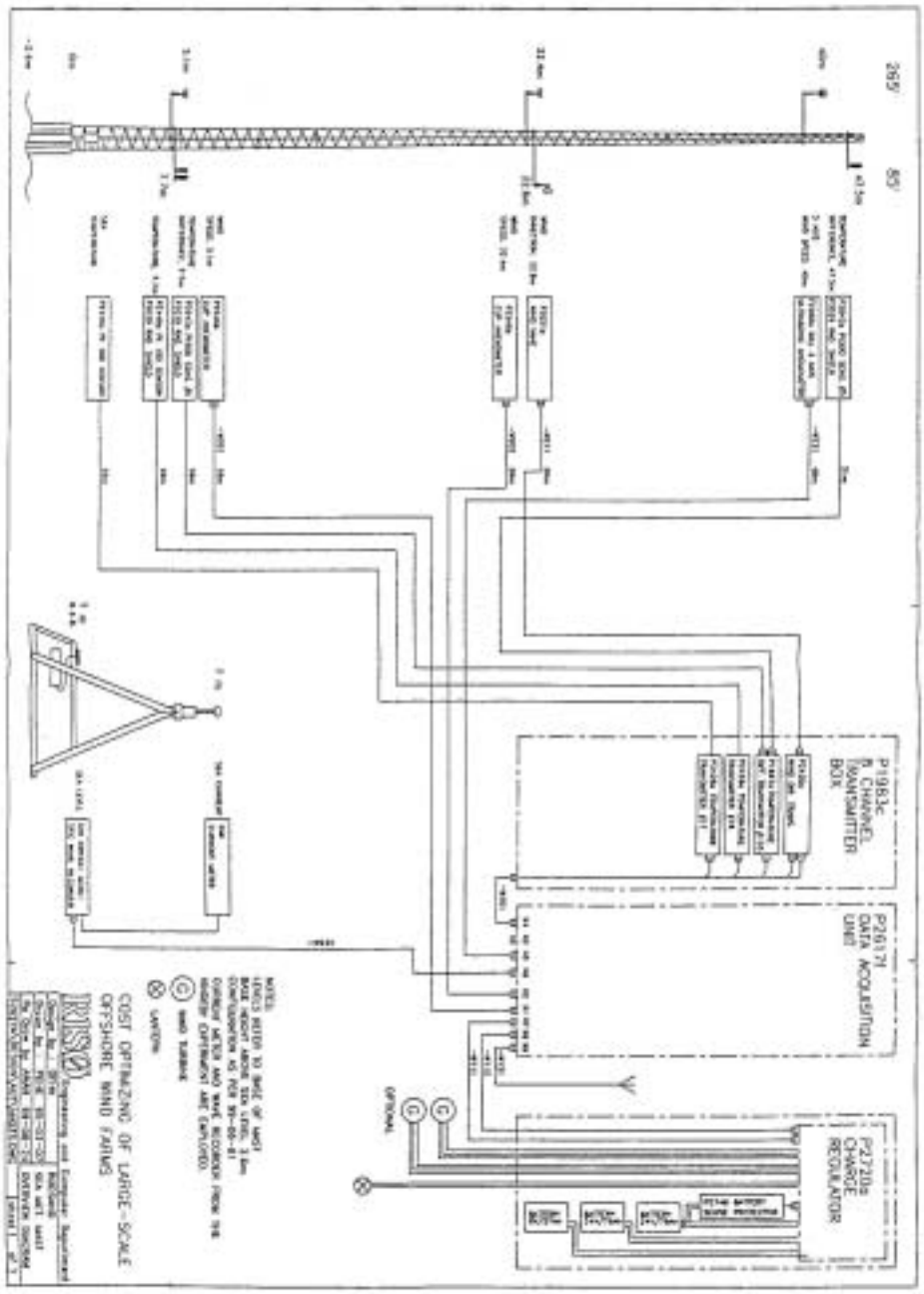

Figure 7: Set-up of the Rødsand mast with the DAQ-system after 5/99

3.3.3 Aanderaa-system

In 5/99 the Aanderaa measurement system was installed additionally to the DAQ-system. Table 4 and Figure 8 show the instrumentation of the measurement mast logged by the Aanderaa system.

Table 4: Instrumentation of the Rødsand measurement logged by the Aanderaa system (after its installation 5/99)

measured quantity	height above mean sea level of 7.7 m	instrument	boom	averaging
Wind speed	50.3 m	cup anemometer	SW	10 min
	29.8 m	cup anemometer	SW	10 min
	29.6 m	cup anemometer	NE	10 min
	10.2 m	cup anemometer	SW	10 min
Wind direction	46.6 m	wind vane	SW	10 min
	27.8 m	wind vane	SW	10 min
air temperature	49.8 m	Pt 500	NE	10 min
	10.0 m	Pt 500	NE	10 min
Temperature difference	49.8 m – 10.0 m	Pt 500	NE	10 min
Sea temperature		Pt 500	-	10 min

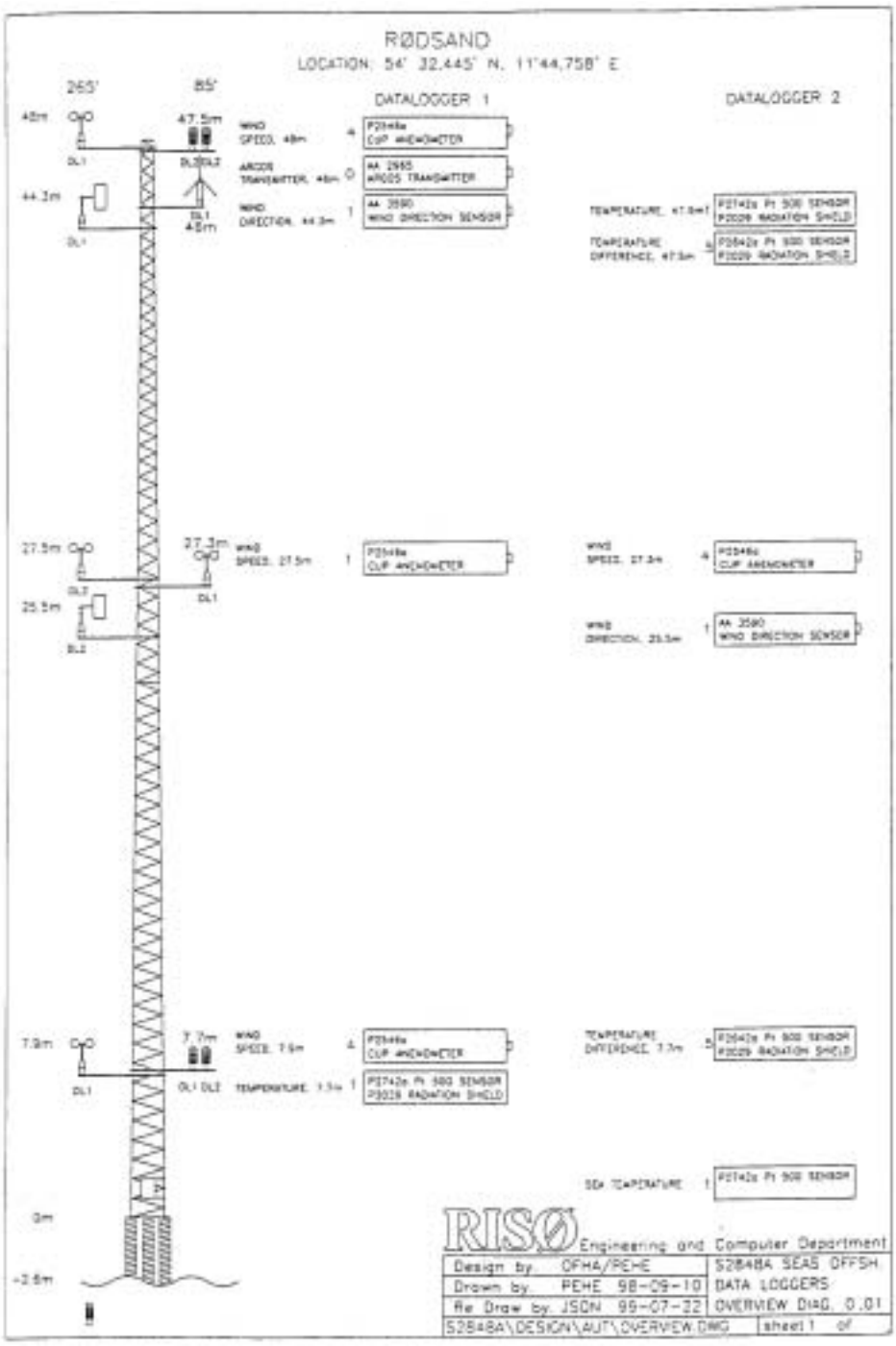

Figure 8: Set-up of the Rødsand mast with the Aanderaa-system

3.4 Instruments

3.4.1 Cup anemometers

Cup anemometers of the type Risø P2546a are used. Prior to their first installation in 10/96 (DAQ-system) or 5/99 (Aanderaa system) they were calibrated in a field calibration. In 5/2000 the cup anemometers of the Aanderaa system were re-calibrated in a wind tunnel to investigate possible changes of the cali-

bration with time and to compare the two calibration methods. The calibration parameters for the field calibration are shown in Table 5 and for the re-calibration in Table 6. Comparison of wind resources calculated using old and new calibrations at Rødsand suggested a difference of 0.08 m/s (the new wind resource estimate being slightly higher) which is within the error margin for the instrument.

Table 5: Field calibration of cup anemometers before first installation

instrument no.	slope	offset
416	0.62440	0.177
417	0.62298	0.185
418	0.62213	0.188
448	0.61871	0.182

Table 6: Wind tunnel re-calibration of the cup anemometers in May 2000 (by WindTest)

instrument no.	slope	offset
416	damaged in transit	
417	0.62243	0.234
418	0.62253	0.230
448	0.61824	0.269

The accuracy of the cup anemometers due to the calibration accuracy is estimated to be +/- 1%. Additionally, for turbulent flows, second order influences such as overspeeding have to be considered. An additional error source is the flow distortion due to the structure on which the anemometer is mounted, i.e. the mast and the booms. Wind direction where the anemometer is in the direct mast shade can not be used. For all other wind directions a correction of the boom effects can be made as shown in (Højstrup, 1999). However, there will always be a remaining uncertainty due to flow distortions.

The overall uncertainty of the wind speed measurement with cup anemometers is estimated to be +/- 3%.

3.4.2 Wind vanes

Wind vanes of the type Risø Aa 3590 were used. The uncertainty of the instrument itself is negligible. However, the adjustment of the orientation of the instrument is difficult in the field. The measured wind directions are calibrated by means of directional turbulence intensity in comparison with the estimated boom direction (see chapter 4.2.4). The absolute accuracy of the wind direction measurement is estimated to be about +/-5º.

3.4.3 Sonic anemometer

The sonic anemometer measures wind speed in three components (x,y,z) in a high resolution of 20 Hz. Additionally the air temperature is measured with the same resolution. It is therefore possible to derive friction velocity and heat flux with the eddy correlation method. The sonic anemometer is of the type Gill F2360a.

In the sonic anemometer the transducers and struts of the instrument distort the wind flow in the measurement volume. This causes a wind direction dependent bias in the measurement (see e.g. (Mortensen and Højstrup 1995). For the horizontal wind speed component a correction for the flow distortions is

made with a calibration curve internally in the instrument. This is not the case for the vertical wind component. This leads to a wind direction dependent bias for the vertical component and therefore also for the friction velocity and heat flux derived from it. The geometry of the instrument with its struts and transducers has a 120° symmetry. By using a 120º sector these errors largely cancel out in the mean value.

The temperature fluctuation response of the instrument is investigated in detail in chapter 4.1.3. The conclusion is that the temperature fluctuation and heat flux measurements can not be used without further analysis, which is outside of the scope of this report.

The mean air temperature measurement has been found to have a temperature dependent bias of more than 1 ºC and should therefore not be used (see chapter 4.2.10).

Measured friction velocities were found to contain spikes which have to be removed (see chapter 4.2.13). The uncertainty in the friction velocity measurement is estimated to be about +/- 10%. This can be improved by using 120º averages.

The estimated accuracy for the horizontal wind speed is about +/- 5% and for the vertical wind speed +/- 8%.

3.4.4 Temperatures and temperature difference

Temperature sensors for air temperature and water temperature were used in addition to a temperature difference sensor. Sensors of type PT100 and PT500 were used. They were mounted with a radiation shield of type P2029.

The temperature difference measurement has a discretisation of 0.0166 K after 5/99.

3.4.5 Acoustic wave recorder

The wave height was measured by an acoustic SODAR-type instrument positioned under water on a support structure on the seabed. The type is the HD-AWR201 from DHI (Dansk Hydraulisk Institut).

Figure 9: Sensor of the acoustic wave recorder

The instrument was located about 100 m south west of the offshore meteorological mast at Rødsand from March 1998 to March 2001. The distance of the instrument to the ground is 3.74 m; the average water level during the measurement was 7.7 m. The distance measured is from the acoustic transducer to the water surface. The sound propagation is straight upwards with an angular spread of 3 degrees. The sound frequency used is 200 kHz and a measurement frequency of 8 Hz is applied.

The cut-off frequency of the instrument is determined by its spatial resolution rather than its sampling rate. The diameter of the sound transducer is about 0.2 m. The measurement area at the water surface is about 0.6 m. Assuming the shortest measurable wavelength is four times the measurement area leads

to a cut-off frequency of about 0.8 Hz.

A fixed speed of sound (1475 m/s) is used independent of actual water temperature and salinity. In general, the speed of sound in water is determined by its temperature, salinity and pressure. The mean salinity for the Rødsand site has been estimated from maps given by (Ostsee-Handbuch, 1978) to 13‰ in February and 11‰ in August. The variation in salinity is expected to have little influence on the speed of sound (less than 1% for 2‰ salinity difference after (Dietrich et al., 1975)). The variation in atmospheric pressure and in water pressure with depth also has negligible influence on the speed of sound. The temperature variation is expected to be most important for variations of the speed of sound. From (Dietrich et al., 1975, p.74) the speed of sound at the surface for a salinity of 12‰ has been estimated to 1420 m/s for 0ºC and 1490 m/s at 20ºC. This leads to the estimated maximum measurement errors of respectively +4% and –1% in the water level value.

In most of the measured time series a fraction of erroneous data points is present, being single data points with random values. As far as possible these were removed by a filter. Records with very high noise levels were rejected. This is described in chapter 4.

The acoustic wave recorder employs limits for the maximum and minimum water level measured to avoid a contamination with second order echoes. These limits were set to a water level of 6.1 m and 8.5 m until November 1999. In November 1999 these limits were changed to a minimum of 5.3 m and a maximum of 10.1 m. Due to a large variation in mean water level these limits were in some cases too narrow to allow an undisturbed wave measurement (see chapter 4).

The instrument measured an absolute time and therefore does not need calibration. The main measurement uncertainty is the dependence of the speed of sound on salinity and temperature, which has not been corrected for. Measurement errors are spikes in the data and data clipping. This can lead to larger uncertainties.

3.4.6 Current measurement

The water current sensor is a two dimensional electromagnetic sensor measuring the water velocity in x- and y-direction, manufactured by GMI (Geophysical and Marine Instrumentation, Denmark). It is located 5.3 m above the sea bottom. The water velocity at this height is composed of both the water movement due to waves and the water current. The mean water current is extracted by averaging and the mean current speed and direction are calculated.

The instrument has been calibrated in a water tank by ‘Sibsteknisk Laboratorium’. The averaged measured parameters of the linear interpolation of 6 flow velocities in 4 directions where a gain of 0.962115 and an offset of

Figure 10: Sensor of the current measurement

0.003616. For different directions and velocities deviation of up to +/- 2% were found.

The instrument can measure velocities up to 150 cm/s. Values above this limit are clipped. A procedure for detecting data series with clipped data has been developed and data with severe clipping have been rejected (see chapter 4).

It is possible that fouling at the site leads to a measurement error. No in situ test or calibration of the instrument has been performed and the influence of this possible error source is not known.

The measurement accuracy of the clean sensor without measurement error is estimated to be +/- 2%.

4 Quality Control

The visual inspection of the data, which is conducted when new data are collected can be seen as the first step in the quality control process. However, further quality control is necessary and is described in this chapter.

The fast sampled data of the sonic, wave and current instruments have been controlled by inspection of time series and spectra of example time series. This is described in chapter 4.1.

The averaged (half-hourly) data have been inspected by their time series and frequency distributions and by making intercomparison between different measured quantities. This also leads to calibrations for the wind and current direction measurements. Investigations of the averaged data are described in chapter 4.2.

4.1 Quality control of fast sampled data

The aim of the QC of fast sampled data is to search for errors and problems in the data, which influence the derived, averaged data and might not be detectable there. Fast sampled data are only stored by the PC based DAQ-system, not by the Aanderaa system. Therefore a QC can only be made for these data.

Fast sampled data are saved with 20 and 5 Hz for the different sensors. The data consists of up to 36000 points per sensor per half hour. Due to this enormous data only very few example data time series could be checked by visual control. For this purpose 12 example time series from different times of the measurement and for different wind conditions were selected (see Table 7). The signals from the three cup anemometers, the wind vane, the sonic anemometer, the acoustic wave rider and the current instrument have been plotted in time series and checked by visual inspection.

The most important parameters from the sonic measurement are the covariances of u'v', which is used to derive the friction velocity and the covariance w'T', which is used to calculate the heat flux. Spectra of u' and w' together with the co-spectrum of u'w', spectra of w' and T' together with the co-spectrum w'T' and additionally spectra of u' and v' together with their co-spectrum have been calculated and plotted for the 12 test data time series.

The main problems found in the quality control of the raw data are described in the following.

4.1.1 Wave data noise and clipping

Two problems have been found in the wave sensor data. Most of the measured time series of water elevations show noise in the form of spikes, i.e. single data points with random values. The instrument is set up with upper and lower limits of measurable water elevations. Measured values are clipped if these values are exceeded.

Spikes

For most of the recorded time series the wave measurement made at Rødsand with the DHI acoustic wave recorder shows spikes in the data. These spikes have a large influence on the measured standard deviation of the water level, which leads to an error in the derived significant wave height. The spikes also have a large influence on the wave spectra.

The noise in the data consists of spikes, i.e. single events of erroneous data points with an almost random value. The spikes occur in a pattern of bursts and within a burst the spikes can form a significant part of the available data. Also a number of spikes can follow each other before a correct data point appears again. There is a tendency for more spikes to occur in situations with higher waves.

All data series therefore have to be filtered to remove these spikes. For this reason an analysis of the wave data is only possible for the measurement periods where the fast sampled raw data are available. Two different types of filters have been tested.

The exponential filter compares each new data point with an expected value. If the difference is smaller than 0.5 m the data point is accepted. Otherwise it is rejected and the last valid data point is used instead. Each time a valid data point x_i is found the expected value x_{expec} is updated with an exponential filter:

$$x_{expec,new}=0.9x_{expec,old}+0.1x_i$$

The adaptive filter is based on the idea of simply comparing each new data point with the last valid one by their difference (or gradient). Unrealistically large gradients are dismissed and the last valid point is repeated instead. The limit for the gradient is dependent on the standard deviation of the first 2000 data points of the uncorrected time series. The limit is enlarged for the number d of consecutive data points, which were dismissed:

$$\text{limit} = 0.17 + 0.5\sigma + 0.03d$$

An example of the despiking of a moderately noisy time series is shown in figure 2. The length of the time series is 40 seconds. The uncorrected data is shown together with the results of the two despiking algorithms. It can be seen that the exponential filter detects all severe spikes and most of the smaller ones. The adapting filter detects even more of the smaller spikes. As a results the corrected time series is only slightly distorted due to undetected very small spikes and the correction of the spikes with a constant value.

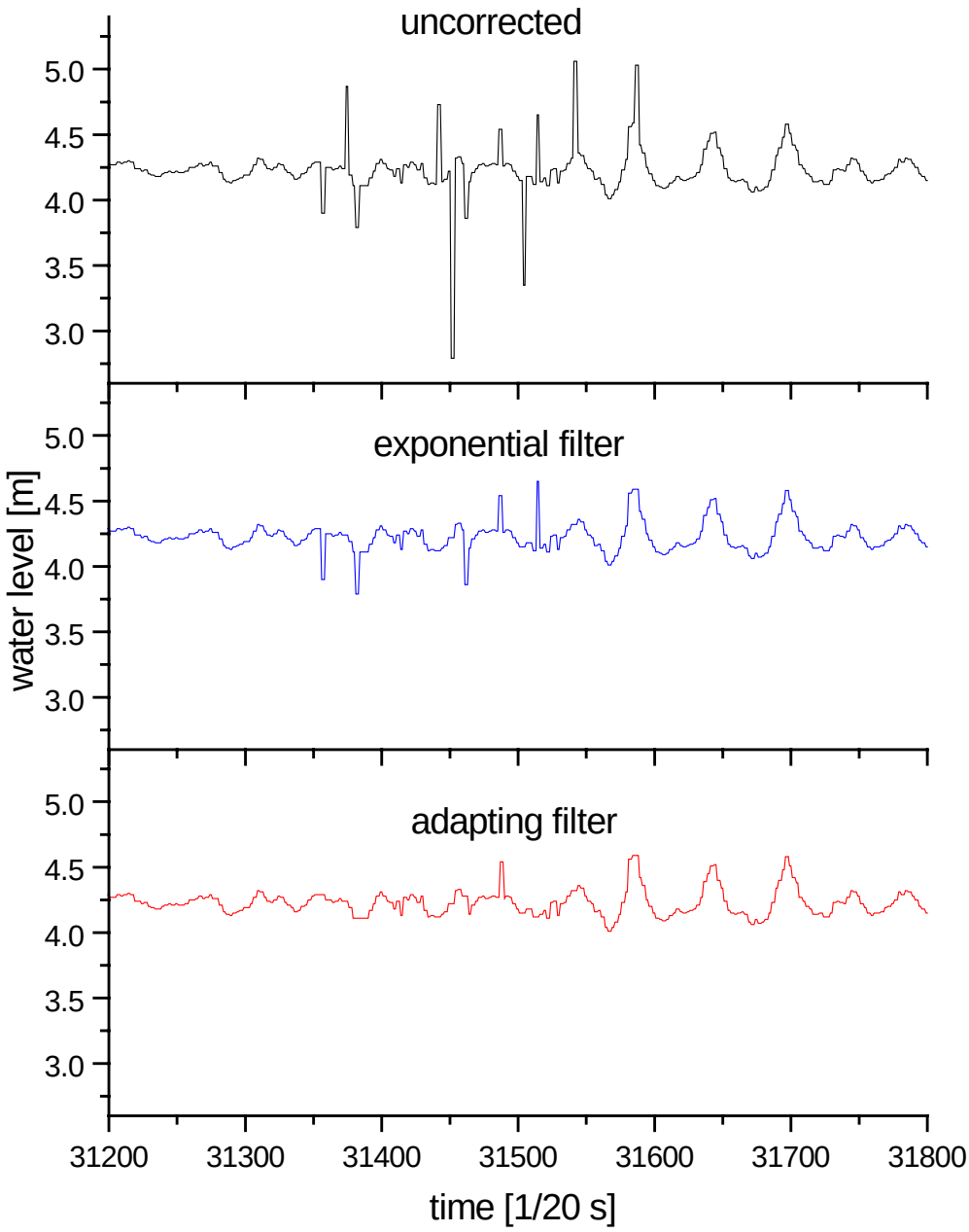

***Figure 2**: Example of the despiking of a moderately noisy time series of 40 s with two different despiking algorithms*

For the same time series the spectra are shown in figure 3. They are calculated by fast Fourier transformation of the 30 minutes measurement record.

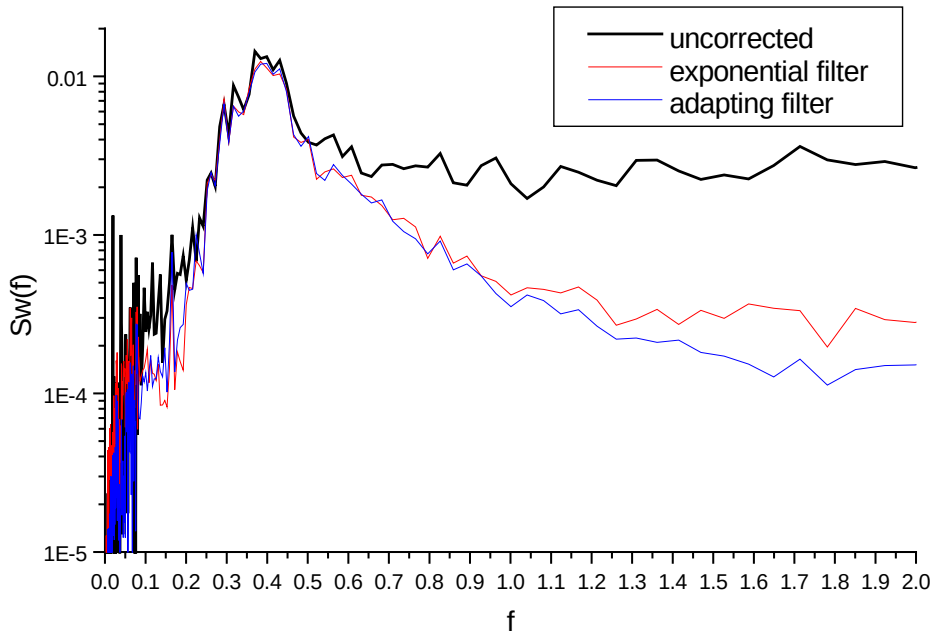

***Figure 3**: Example of the effect of the despiking on the spectrum of the time series shown above. 30 min data have been used for the spectrum*

It can be seen that the spikes in the data result in spectral components for frequencies higher than 0.5. The remaining small spikes in the time series corrected with the exponential filter still have an influence on the spectrum for frequencies exceeding 0.8 Hz. Therefore it can be assumed that also the last few remaining spikes in the correction with the adapting filter will slightly distort the spectrum for higher frequencies. But since the resolution of the acoustic wave recorder is only approximately 1 Hz these higher frequencies have to be disregarded anyway.

The adapting filter has been chosen for the correction of the wave measurements. However, it was found that in some cases the noise level is too high to make a sensible correction of the data.

As an example for severe measurement noise the measurement during the storm on 3.12.1999 for the time 21:30 to 22:00 is shown. The wind speed at 10 m height was 24 m/s. The wave record is shown in Figure 11. The measurement consists almost completely of noise and a signal can only very occasionally be detected. An estimation of wave height or even the water level is impossible.

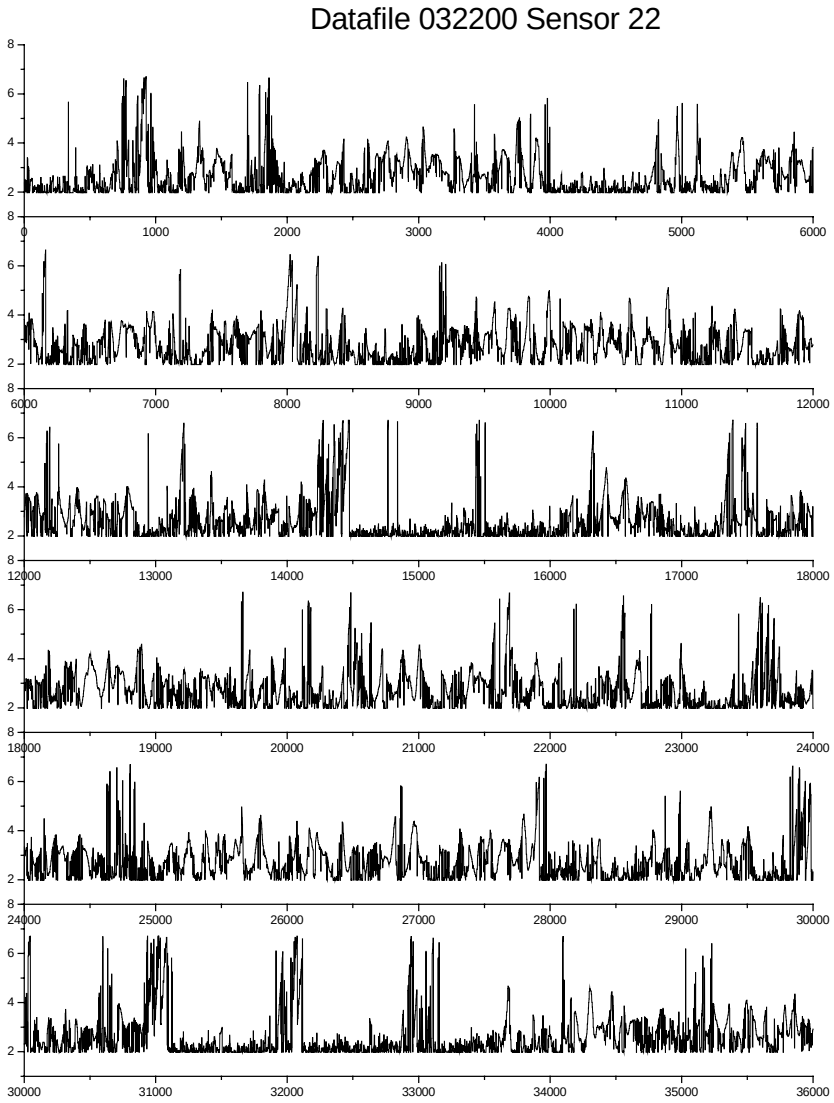

Figure 11: Water level record on 3.12.1999 21:30 to 22:00; shown is the water level above the instrument versus record number with a sampling rate of 20 Hz (each of the 6 plots shows a time period of 5 minutes); no correction has been applied

As an indication of the noise level of a measurement record the number of spikes detected by the adapting filter in each record is counted. A maximum acceptable level of noise has been established by visual inspection of the example time series. The result is shown in Table 7. It was estimated that the filtered signal could not be used for time series where more than 1500 spikes were detected. Time series with a higher noise level have been omitted.

Table 7: Result of filtering of example wave data (++=no problem, +=can be used, -=should not be used, --=not usable)

	Date and time (YYY-YMMDDhhmm)	no of errors found	result of visual inspection
spring 1998	199804030000	1283	++
	199804031200	1171	+
	199804100000	881	++
	199803220000	593	+
1999 before wave instrument up-grade	199902050000	3286	--
	199902190000	542	+
	199906150000	295	+
1999 after wave instrument up-grade	199912032200	8749	--
	199912031800	5886	-
	199912031400	2336	-
	199912010000	1088	++
	199911290000	463	++

The reason for the noise in the data is not known. However, it can clearly be seen that the level of noise in the data increases with increasing wave height or wind speed. A possible explanation is the presence of foam from breaking waves. Extreme waves with pure spray are likely not to be detected by the acoustic wave sensor. It's advantage is the accurate detection of small waves which might be important for the sea surface roughness. For extreme wave measurement other types of sensors should be used, e.g. pressure cells or wave rider buoys. (personal communication Ole Peder Clausen, DHI, 31.7.2000).

Measurement limits

The instrument set-up of the wave recorder includes values for the minimum and maximum water level possible. This behaviour leads to problems for large waves occurring at a low or high water level. Here the measurements are clipped off at a certain water level.

In November 1999 the wave sensor was repaired and updated and the upper and lower limits of valid measurement data have been broadened to avoid data clipping. Measurement limits have been changed from 6.1-8.5 m to 5.3-10.1 m. The new limits have been installed successfully and a broader range of water levels can be measured since 11/99.

An example time series is shown in figure 4. The uncorrected data is shown together with the results of the two despiking algorithms. It can be seen that the water level measurements of the time series are clipped at the lower measurement limit due to high waves at relatively low water level. The data series shows that some of the clipped values are reflected to the upper measurement limit. The resulting time series is heavily distorted due to the clipping of the wave data. Also there are still spikes and other errors present.

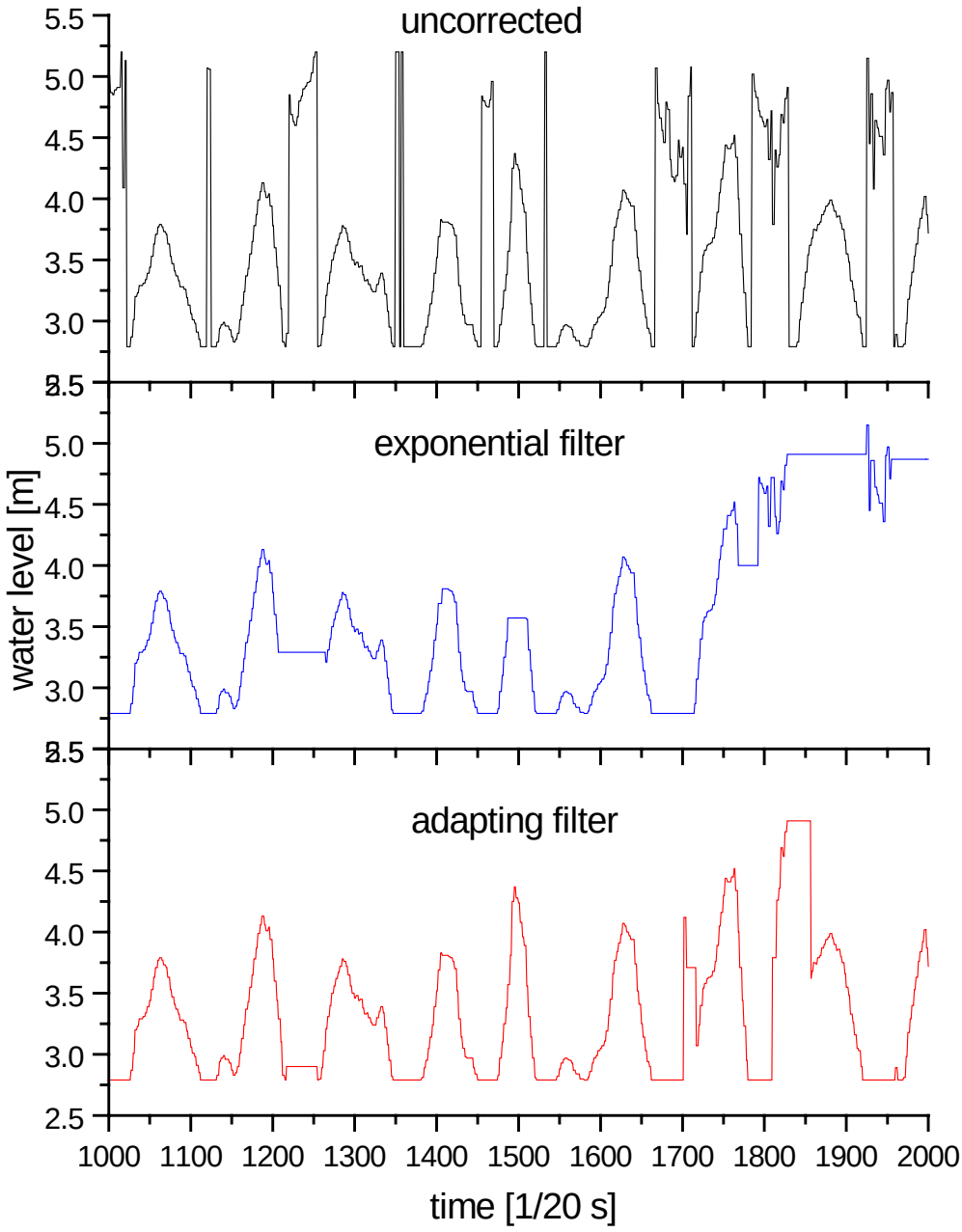

***Figure 4**: Example of a time series (50 s) clipped off due to the set-up of the minimum water level value*

4.1.2 Current data clipping

The current measurement records the velocity of the water at a point 1.56 m above the wave sensor, e.g. 5.3 m above the sea bottom. The current is measured in two components in x- and y- direction.

The current meter measures the combination of mean water current and water velocity due to wave action. At high velocities near the top and crest of high waves the current sensor shows erroneous short (up to about 2 s) periods of constant current. This has been found very occasionally at the 199912031800 time series and more pronounced at the 199912032200 time series. It is estimated that the error occurs up to about 10% of the total measurement time. The

reason for this error is the measurement limit of 150 cm/s set for the current instrument (personal communication Ole Peder Clausen, DHI, 31.7.2000).

This problem only occurred in two of the test time series. The number of occasions with constant current reading is determined and data with a large amount of errors are omitted.

Figure 12 shows the measurement record for the y-component of the water movement on the 3.12.1999 at 21:30 to 22:00. The mean wind speed was about 24 m/s at 10 m height. It can clearly be seen that the measured water velocity is clipped at a level of approximately 150 cm/s. All records higher than this seem to have been disregarded and the record shows a constant velocity instead.

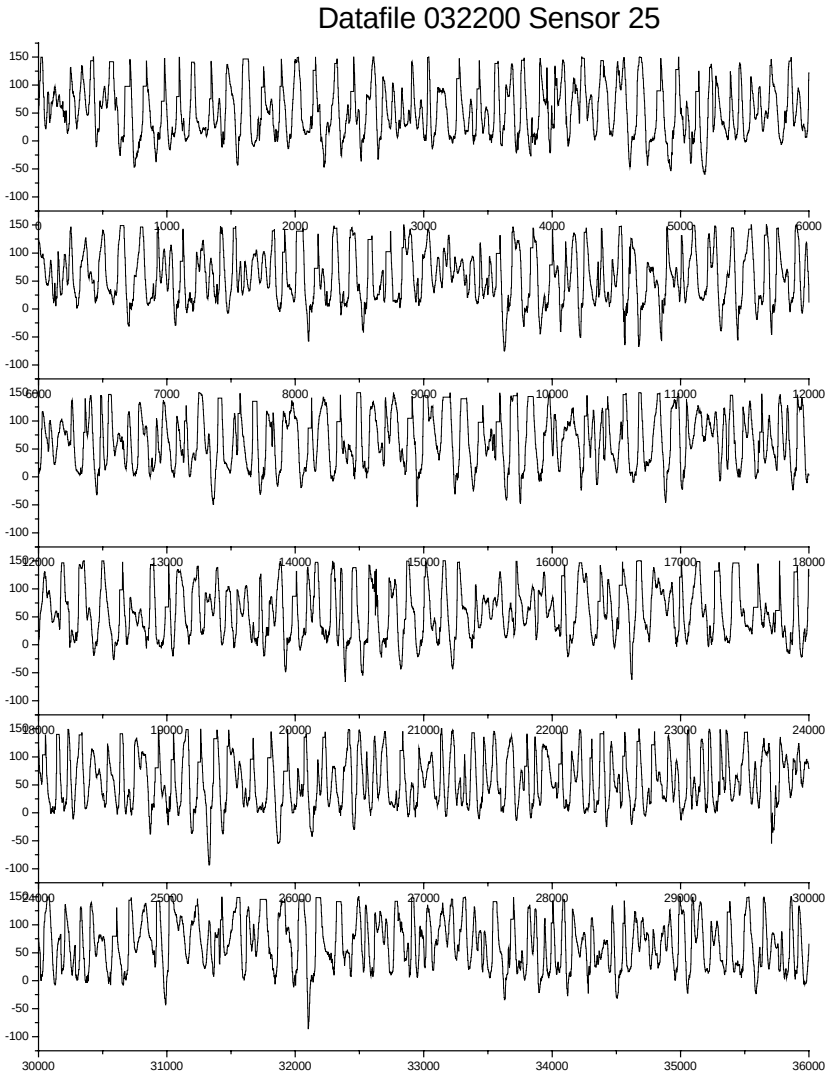

Figure 12: Water current record in y direction on 3.12.1999 21:30 to 22:00; shown is the water current in cm/s versus record number with a sampling rate of 20 Hz (each of the 6 plots shows a time period of 5 minutes)

To detect errors of clipped data the number of occurrences of measurement periods without change of the measured value were recorded for the two components. There can be two reasons why the measured current does not change for several consecutively measured samples:

- the data is clipped because of a measurement limit – this will occur for high speeds
- the current is temporarily completely constant within the measurement resolution – this will occur for small currents.

Figure 13 shows the number of occurrences versus component speed. It can be clearly seen that the 'no change' condition occurs often at low speeds for the x-component. This is probably a sign for a constant current and no measurement error. For the y-component it occurs also for high speeds. This is believed to be due to data clipping. Data with more than 3 occurrences of the 'no change' condition for the y-component are omitted.

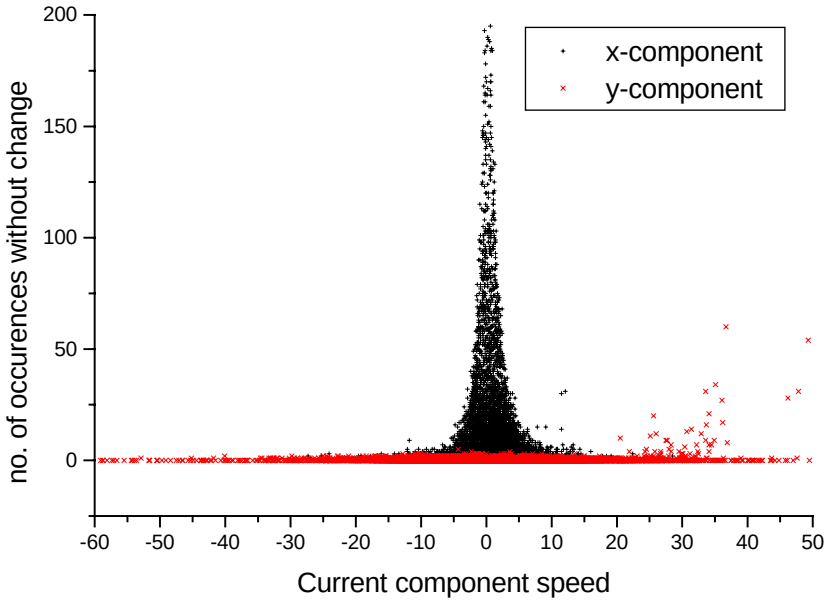

Figure 13: Number of occurrences of measurement periods without change of the measured value versus current component speed for the two components

4.1.3 Noise in sonic signals

The signals of the sonic anemometer have been inspected both in the time domain as time series plots and in the frequency domain as spectra and co-spectra.

From the time series is can be seen that some data series show spikes, i.e. single erroneous data points. All sonic data therefore have been filtered for spikes.

A statistical data screening procedure assuming normal distribution of data has been used. It compares each data value with a forecast value and replaces the measured value by the forecast value if the difference between both is too large. The statistical screening procedure is described in [Højstrup 1993].

The method has been tested with the example data series. The result is shown in Table 8. The number of spike found by the filter is close to what would be expected from the time series plots, although clearly not all spikes were found.

Table 8: Number of spikes detected in the sonic data

	Date and time (YYY-YMMDDhhmm)	spikes detected in x-signal	spikes detected in y-signal	spikes detected in z-signal	spikes detected in T-signal
spring 1998	199804030000	-	-	-	1
	199804031200	-	-	-	-
	199804100000	-	-	-	-
	199803220000	-	-	-	-
1999 before wave instrument upgrade	199902050000	-	-	2	-
	199902190000	-	-	-	-
	199906150000	-	-	-	-
1999 after wave instrument upgrade	199912032200	-	5	2	-
	199912031800	-	-	-	3
	199912031400	-	-	-	1
	199912010000	-	-	9	2
	199911290000	-	-	-	-

Already in the time series plots - sometimes intermittent - high frequency oscillations are visible in some signals. These are investigated further by means of spectra and co-spectra of the signal.

The u', v' and w' signals occasionally show peaks, which are probably due to oscillations of the support structure or the instrument itself. However, except for very low wind speeds these peaks only contribute with a small part of the total variance and the signal can be used if some measurement uncertainty is accepted.

The T' signal shows a high noise level and is often additionally contaminated by peaks. It is concluded that the T' signal and the w'T' co-spectrum can not be used without further analysis and filtering, e.g. also no heat flux can be derived.

A further investigation of the dynamic behaviour of the mast and boom structure and the sonic anemometer itself could explain the peaks found in the spectra. The findings of this should then be compared to a more thorough investigation of peaks in the measured data. However, this is outside the scope of this quality control.

Two examples in Figure 14 and Figure 15 show a peak in the temperature spectrum and noise at high frequencies, respectively.

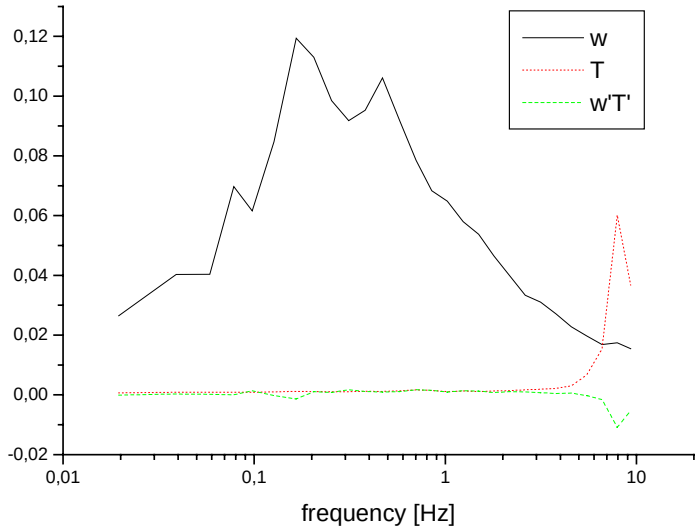

Figure 14: Spectra of w and T signal from the sonic anemometer and w'T' co-spectrum for the data time series 19991201000

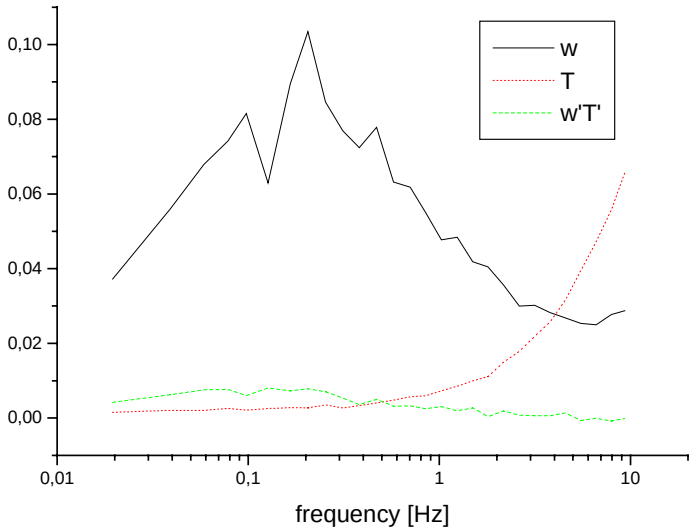

Figure 15: Spectra of w and T signal from the sonic anemometer and w'T' co-spectrum for the data time series 199912031400

4.2 Quality control of statistical data

The processing of raw data to statistical data is described in chapter 5. The time series of the parameters used for the data file have been quality controlled by visual inspection of plotted time series, histograms and comparative scatter plots for several pairs of parameters. The results are described in the following paragraphs.

4.2.1 Mean wind speeds

Four measurements of mean wind speeds are available: 3 cup anemometers at heights 10.2m, 29.8m and 50.3m and the sonic anemometer at 46.6m (later 42.3m).

The frequency distributions of these measurements are shown in Figure 16. The increase of wind speed with height is clearly visible. The distributions of the sonic and the highest cup anemometer are as expected quite similar.

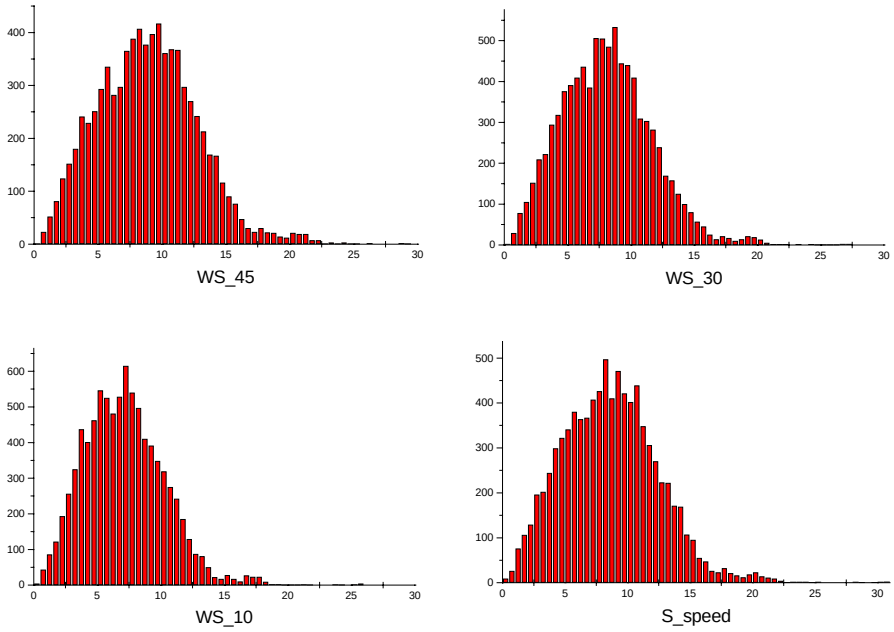

Figure 16: Frequency distribution of measured wind speeds from (a) cup anemometer at 50.3 m, (b) cup anemometer at 29.8m, (c) cup anemometer at 10.2m and (d) sonic anemometer at 46.6/42.3m

A better comparison between the different parameters can be made by scatter plots of measured wind speeds against each other. These are shown in Figure 17. Completely incoherent measurements, which would be the result of malfunctioning instruments, can not be found. However, there are some considerable deviations in the ratios of the measurements in different heights from a simple logarithmic profile. This can also be seen very clearly in the time series plots, where for some time periods the measurements at different heights show almost the same wind speed, while at other times a large vertical wind speed gradient can be seen. There are several reasons for this:

- Temperature stratification is clearly the most important influence. This can be seen clearly by comparing the wind speed time series with the temperature difference time series. Almost always there is a relation between a negative temperature difference (unstable stratification) and a small vertical wind speed gradient and vice versa.
- Instationary situations, e.g. times of a significant weather shift with a large wind direction change, sometimes seem to disturb the vertical wind speed profile for a short time.
- The mast shadow might have a different influence at different heights and therefore disturb the wind speed ratios. It can be clearly seen from the time series plots that many situations with a wind speed at 50 m measured lower than at 30 m were correlated with wind directions around 90 degrees, which is where the mast is shading the anemometers. The reason might be that the boom directions or the wind directions at the two heights were

slightly different. Also the presence of the rod for lightning protection at the top of the mast might have an influence. Measurements where the anemometer is in the direct mast shadow should be omitted.

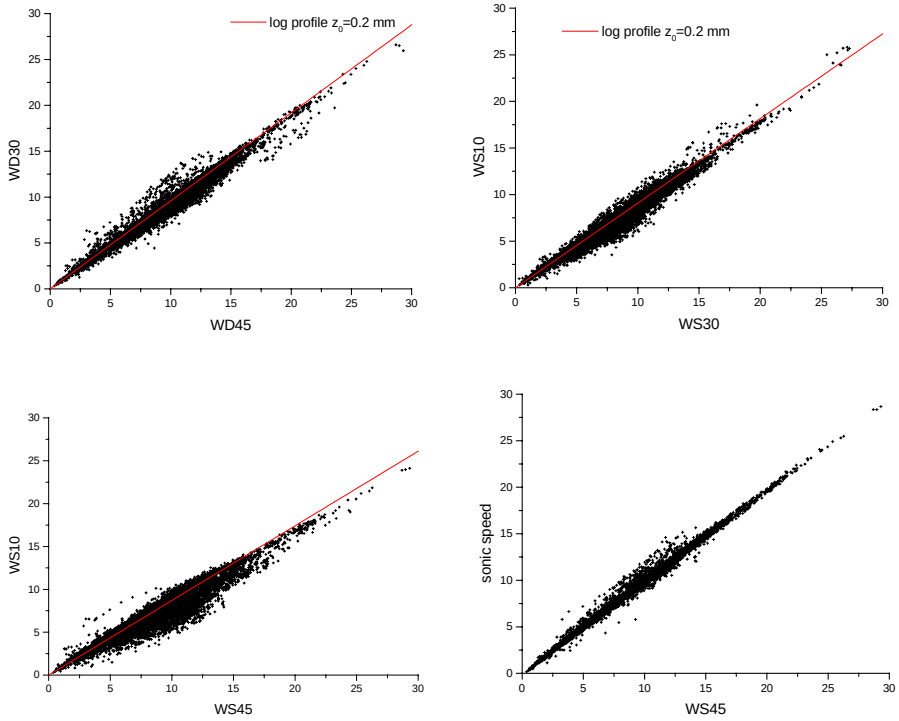

Figure 17: Scatter plots of measured wind speeds before QC

4.2.2 Wind speed standard deviations and turbulence intensities

Wind speed standard deviations and turbulence intensities are usually calculated for time periods of 10 minutes. Here the time series of 30 minute averages is used. Therefore the measured standard deviations are larger, especially if the wind speed is changing during the period of the time series. This can clearly be seen in the plotted time series, where the standard deviations for some single values are much higher than for the surrounding values. These single high values can almost always be identified as wind speed changes in the wind speed time series. Looking at turbulence intensities one should be aware of this problem of instationarities in the wind speed which have a large influence on the measured turbulence intensity, especially with the long averaging time of 30 minutes used here. This can also be seen in the histogram plots shown in Figure 18 and Figure 19. Turbulence intensities up to 30% have been recorded. It is very likely that most of these high values are actually due to wind speed changes.

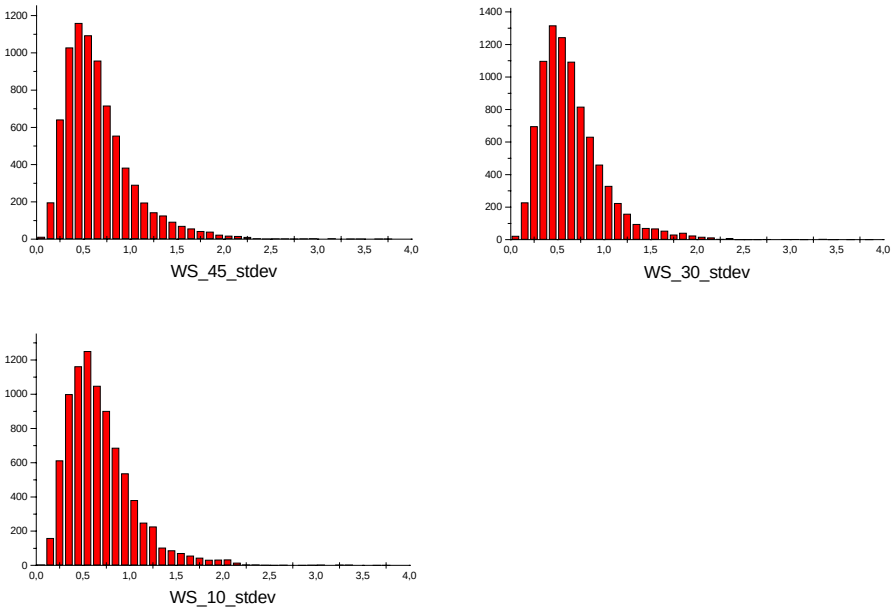

Figure 18: Histograms of measured standard deviations of the wind speed at different heights at Rødsand

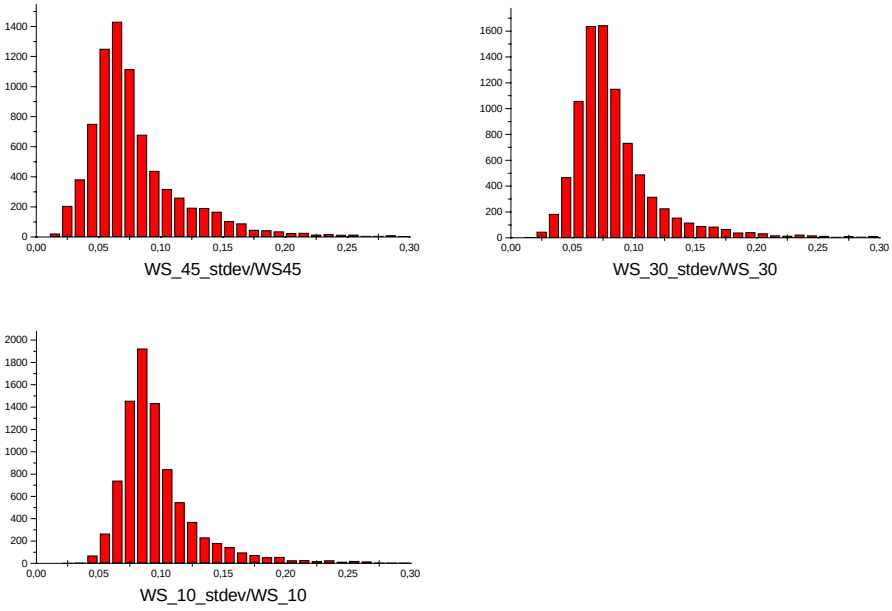

Figure 19: Histograms of measured turbulence intensities at different heights at Rødsand

4.2.3 Wind speed gust values

The time series of gust values of the measured wind speeds reflect very much the wind speed time series themselves. This can also be seen at the histograms, which are shown in Figure 20. Apart from the higher values they are very similar to those of the wind speeds.

The ratio of the maximum measured wind speed and its mean value are shown for the different heights in Figure 21. For the measurement at 50 m height (WS45) a large number of records with value 1 appears. This is a result of the

period where this anemometer was not working and all values were set to the same error indicator. Otherwise the distributions are similar to those of the turbulence intensity.

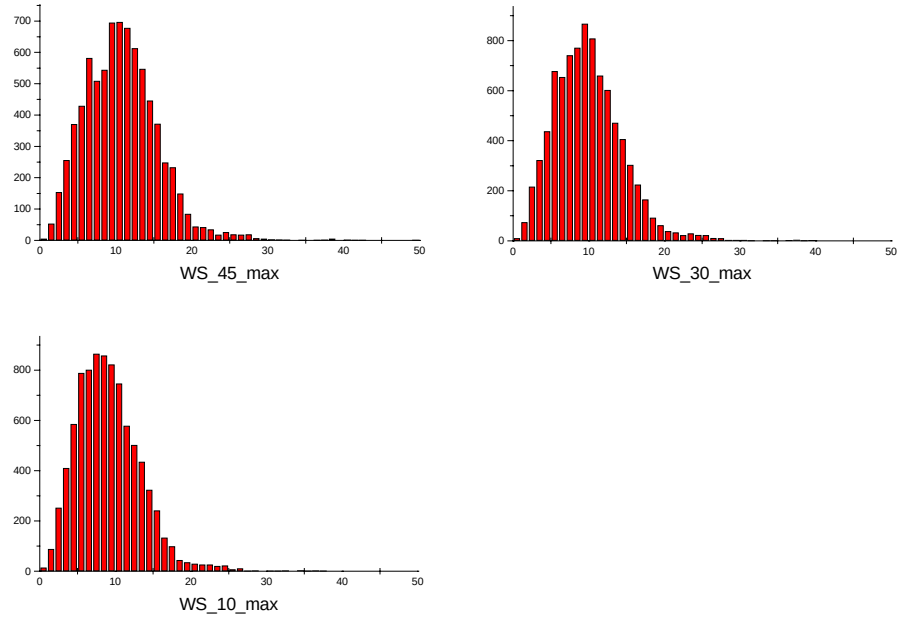

Figure 20: Histograms of measured maximum values of the wind speed at different heights at Rødsand

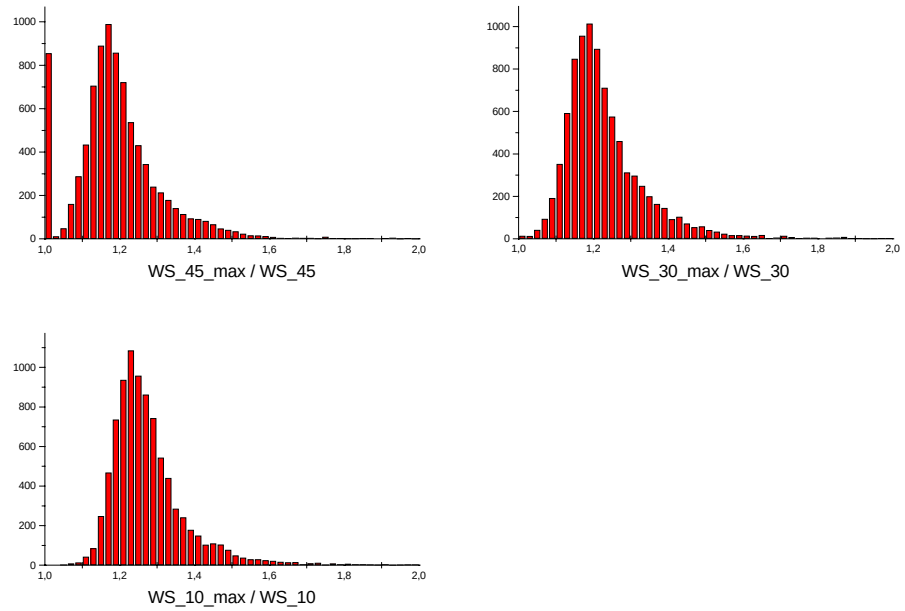

Figure 21: Histograms of measured ratio of maximum to average wind speed at different heights at Rødsand

4.2.4 Wind directions

Two wind direction sensors are employed at Rødsand: a wind vane at 30m (later 28m) height and the sonic anemometer. A look at the time series plots reveals that there is a nearly constant difference between the two measured wind directions. This can also be seen from the histograms shown in Figure 22.

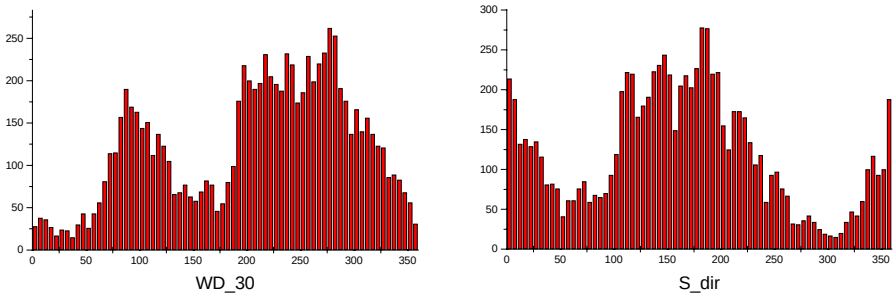

Figure 22: Histograms of measured wind directions at Rødsand

The wind direction sensors (and sonic anemometer) have to be calibrated from the measured data since a correct alignment of the instrument is difficult in the field. The relative calibration has been done by comparing different sensors. For the absolute calibration the mast shadow effect is used as an indication of the boom direction, which has been estimated. However, this calibration procedure should not be expected to give an absolute accuracy of better than 5°. Since all instruments were remounted at the change of the set-up it is necessary to do the calibrations for both set-ups separately.

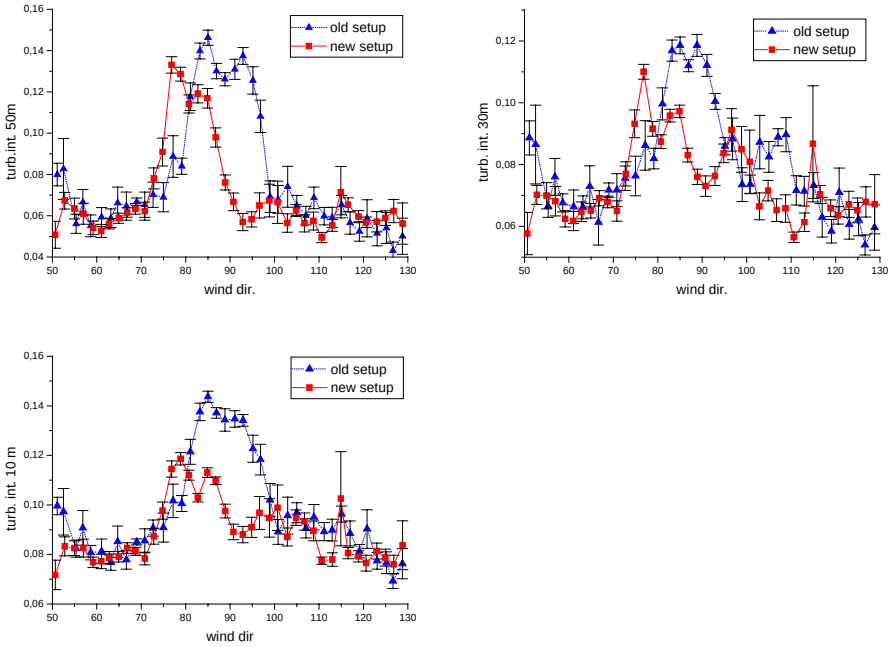

Figure 23: Turbulence intensity measured at the three cup anemometers at Rødsand versus wind direction measured with the wind vane for the old (until May 1999) and new measurement set-up

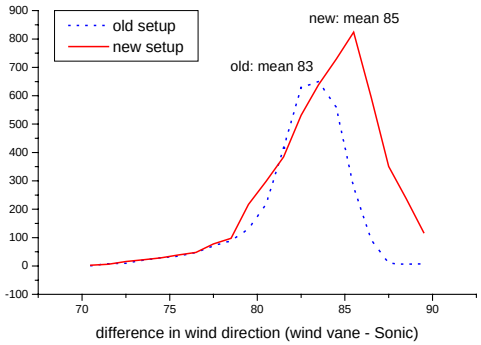

Figure 24: Histogram of differences in wind direction measurement between wind vane and Sonic anemometer

Figure 23 shows the bin averages of the turbulence intensity of the three cup anemometers versus wind vane wind direction for the directions around the mast shade. Both the old and new set-up are shown. A clear increase in turbulence intensity due to mast shadow effects can be seen. For the old measurement this is located around the estimated boom direction of 85°. For the new measurement the measured wind direction is about 5-10° smaller. Therefore a calibration of +7° has been made for the new set-up.

For the sonic anemometer no standard deviation parameter is readily available. It is calibrated by comparison with the wind vane. Figure 24 shows the frequency distribution of differences between the two wind direction sensors. A mean difference of 83° for the old set-up and 85° for the new set-up was found. For the new set-up a combined correction for the wind vane and the Sonic anemometer has to be used since the difference for the new set-up is relative to the wind vane of the new set-up. The correction parameters found are shown in Table 9.

Table 9: Corrections for the wind direction measurements

set-up	instrument	correction
old set-up until May 1999	wind vane	0°
	Sonic anemometer	+83°
new set-up since May 1999	wind vane	+7°
	Sonic anemometer	+92°

Measurements in the direct shade of the measurement mast are severely disturbed and have to be omitted. From Figure 23 it can be estimated that the main disturbance is for a sector of (calibrated) wind directions 70°-110°.

4.2.5 Mean sea level

Time series plots of the mean sea level signal reveal two kinds of erroneous readings: variations in the signal that are traceable to spikes and erroneous single values when a measurement was disrupted. The first can be detected by the number of spikes found by the despiking procedure. Records with more than 1500 detected spike values were disregarded (see chapter 4.1). The second error is present in all wave parameters, e.g. significant wave height and especially the wave periods show unrealistic values. With an upper limit of 7 s for the wave period T50 these errors can be found and for records with higher values all wave sensor values have to be omitted.

Due to the measurement limits of the wave sensor discussed in chapter 4 there is a lower and upper limit of measurable mean sea level. Before the wave instrument upgrade in November 1999 there was one occasion on the 4. and 5.2.99, where the measurement was erroneous due to the lower measurement limit. Here the lowest measured mean sea level value was about 7.0 meters. With the instrument upgrade the measurement window was broadened and on the 1.12.99 a mean sea level of about 6.3 meters was measured. However, also here the lower measurement limit was reached and the measurement showed erroneous values for a short period of time.

The histogram of the mean sea level measurement is shown in Figure 25. It should be noted that the range from 6 to 7 meters MSL was only measurable for a short part of the measurement since November 1999. Therefore the frequency of occurrence can be underrepresented here.

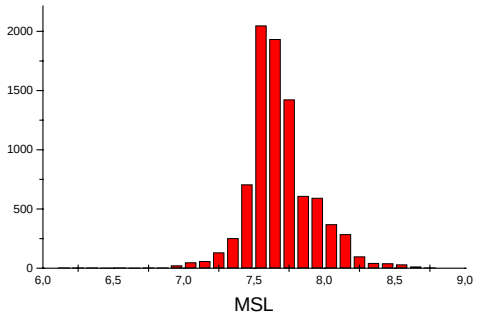

Figure 25: Histograms of measured mean sea level at Rødsand

The mean value of the MSL for all valid measurement records is 7.69 m (standard deviation of the mean 0.002 m). If only measurements at low wind speeds (<5 m/s at 10 m height) are used the mean of the MSL is equally 7.69 m with a standard deviation of the mean of 0.004 m.

4.2.6 Significant wave height

The significant wave height is derived from the standard deviation of the water level measurement. From the time series plots the same two types of errors as for the mean sea level can be found. They are detected by the spike detection procedure and the limit in wave period measurements as discussed there. The histogram of significant wave heights measured at Rødsand is shown in Figure 26.

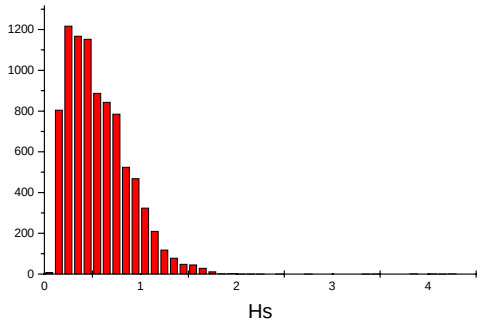

Figure 26: Histograms of measured significant wave height at Rødsand

4.2.7 Wave periods

Three different wave periods are derived from the wave spectrum calculated for each 30 minute wave record measured at Rødsand:

- the wave period at 50% variance T50
- the mean period (m0/m1) Tm
- the mean period based on zero crossing frequency (sqrt(m0/m2)) Tz.

Additionally the bandwidth of the wave spectrum is calculated as ($\log_{10}(f_{75}/f_{25})$). Here m_n denotes the nth moment of the spectrum and f_n the frequency at n% variance.

The concept of a single wave period that is calculated from the properties of the wave spectrum is only valid for a single peaked spectrum. The bandwidth gives an indication for this. It is a measure for the broadness of the spectrum, e.g. double peaked spectra would be detected as very broad spectra with a high bandwidth. However, it is not possible to distinguish between a double peaked spectrum and a single peaked spectrum, which is broad because of e.g. decaying waves.

From the time series plots of wave periods and bandwidth a clear connection between irregularities in the wave period measurement and the measured bandwidth can be seen. Measurements with a bandwidth of more than 0.25 have to be omitted to avoid erroneous values due to double peaked spectra.

The histograms of the three wave periods are shown in Figure 27. The histogram of the bandwidth can be seen in Figure 28. It shows a clear maximum at about 0.17 with an almost symmetric distribution around it up to values of 0.2. A very long tail is found for values above this. This is partly due to double peaked or other transitional spectra.

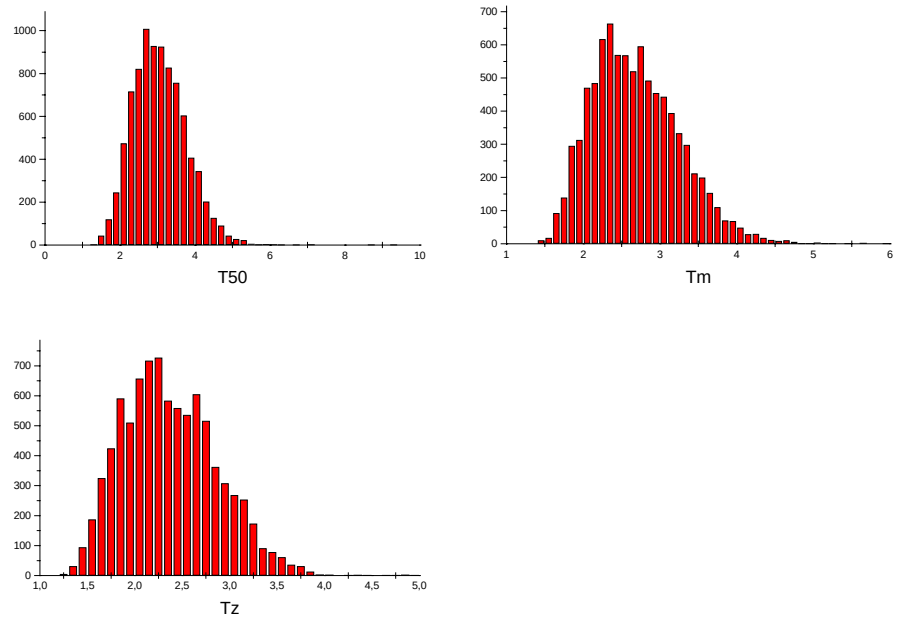

Figure 27: Histograms of measured wave periods at Rødsand; T50 is the wave period at 50% variance, Tm is the mean period (m_0/m_1) and Tz is the mean period based on zero crossing frequency (sqrt(m_0/m_2))

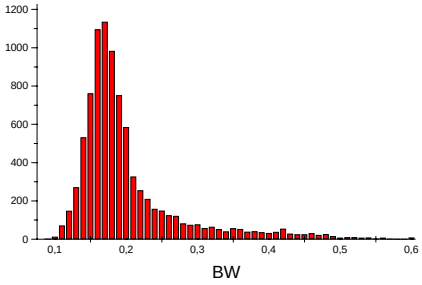

Figure 28: Histograms of measured bandwidth of the wave spectrum ($log_{10}(f_{75}/f_{25})$) at Rødsand

4.2.8 Current speed

The water current is measured in two components x and y by an electromagnetic sensor. It is then converted to a current speed and a current direction. The time series of the current speed does not show any obvious errors or disturbances. The histogram is shown in Figure 29. It shows a long tail of low probabilities for very high currents.

To detect errors of clipped data the number of occurrences of measurement periods without change of the measured value were recorded for the two components (see chapter 4). Data with more than 3 occurrences of the 'no change' condition for the y-component (Cur-err2) have to be omitted.

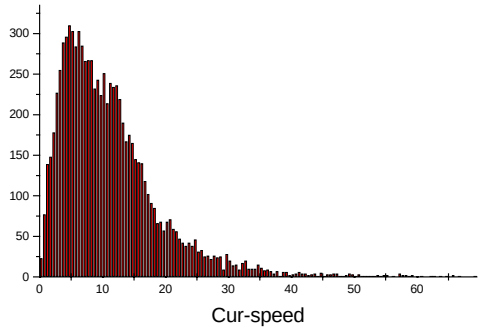

Figure 29: Histograms of measured current speed (in cm/s) at Rødsand

4.2.9 Current direction

The current direction is derived from the two components of the current measurement. It is as usually given as the direction the current is flowing TO (opposite to the convention for wind directions, which are given as the direction the wind is blowing FROM).

The histogram of current directions is shown in Figure 30. Two main directions along the coastline are very prominent. A scatter plot of current and wind direction is shown in Figure 31, where cases with low wind or current have been omitted. Here the current direction is shown with the same convention as the wind direction, e.g. 180° is subtracted. It can be seen that the two most frequent current directions are often connected to wind directions, but also the case of current running against the wind can be found.

As the wind direction, also the current direction has to be calibrated. Here a compass in the current instrument gives the alignment of the instrument. The direction given by the compass has been checked by divers when installing the

instrument. They reported an alignment of 190° with the compass giving 188°. Therefore the compass is used despite the problem that the instrument is standing on an iron support structure which can disturb the compass measurements. The values for the calibration is given in the data and varies between 188° and 205° due to slightly different installations of the instrument before and after the upgrade from November 1999. All current direction data have to be calibrated with the compass data.

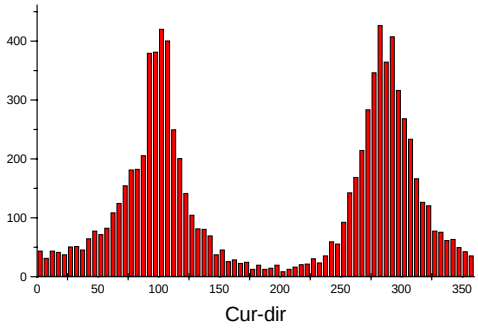

Figure 30: Histograms of measured current direction (direction from *which the current is coming) at Rødsand (only roughly calibrated 180°)*

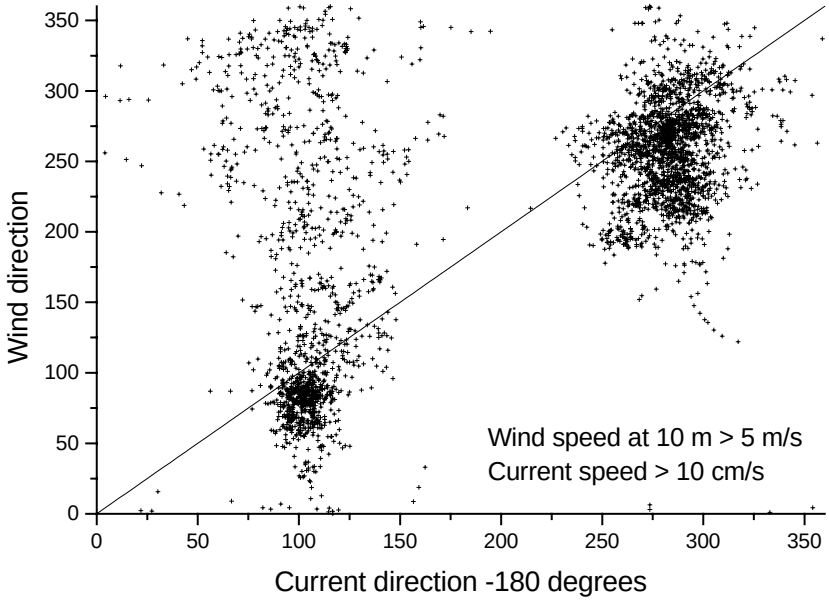

Figure 31: Scatter plot of wind and current direction at Rødsand; only cases with wind speed at 10 m height larger than 5 m/s and current larger than 10 cm/s are shown; shown is the direction opposite the current direction, e.g. both wind and current are given as the direction they are coming from (only roughly calibrated 180°)

4.2.10 Air and sea temperatures

Three absolute temperatures are measured at Rødsand: the air temperature is measured at 10 m height with a PT100 sensor and at 46.6/42.3 m height with the sonic anemometer. The water temperature is measured with a PT 100 sen-

sor. The time series of the measurements show that the water temperature usually changes only very slowly with time. However, there are a few occasions in summer when the water temperature changes by 1-2ºC within a few hours. Frequency distributions of air and water temperature measurements are shown in Figure 32 and Figure 33, respectively.

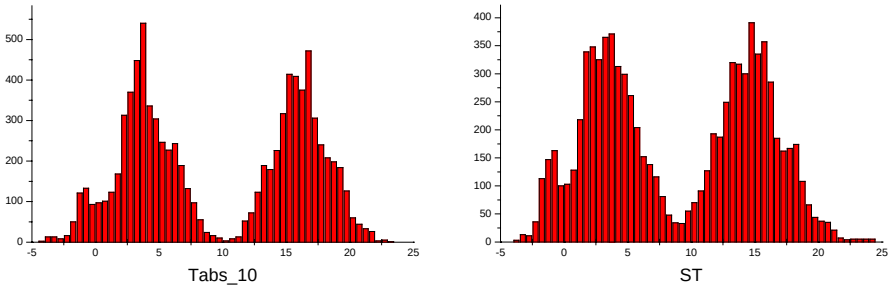

Figure 32: Frequency distributions of air temperatures measured with the PT100 sensor at 10 m height (left) and with the sonic anemometer (right)

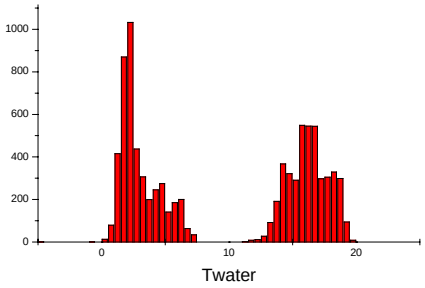

Figure 33: Frequency distribution of water temperature measured with the PT100 sensor

A comparison between the two air temperature measurements is shown in Figure 34. The scatter plot shows rather large differences between the two temperatures. This is partly due to the actual temperature difference at the two heights and partly to a temperature dependent bias in the sonic temperature measurement and will be discussed in the next chapter.

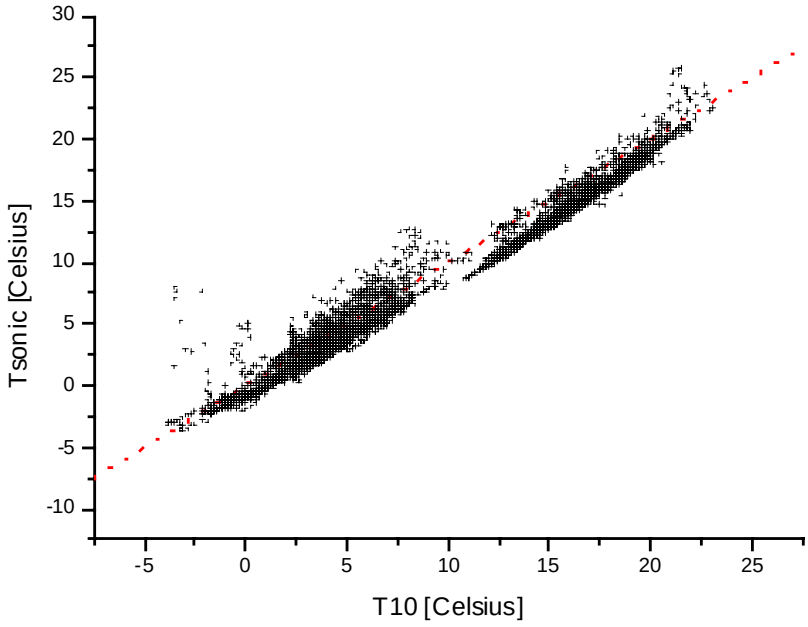

Figure 34: Scatter plot of air temperatures measured with the sonic anemometer at 46.6/42.3 m height versus the one measured with a PT100 sensor at 10 m

4.2.11 Temperature difference

The difference in air temperature between 10 m and 50 m height has been measured by a pair of two PT500 sensors.

Figure 35 shows the frequency distribution. The maximum visible in the bin centred at 0.1 ºC is due to an instrument failure in the time period 26.3.-1.6.1999, where the instrument was first giving random values and later a value of about 0.1 ºC. This also explains some of the extremely high values.

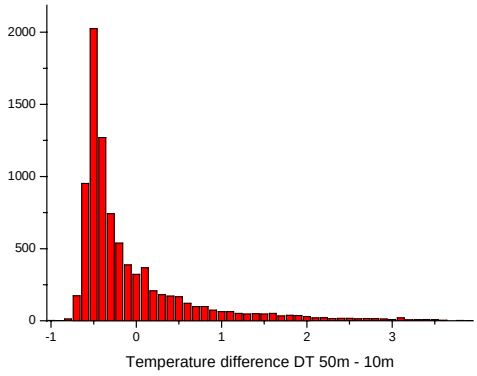

Figure 35: Frequency distribution of the air temperature difference measurement between 10 and 50 m

An air temperature at the height of the sonic anemometer has been estimated using the measured air temperature at 10 height and the temperature difference measurement. This is compared with the temperature measured by the sonic in Figure 36. Generally a better comparison is found than in Figure 34 where only the 10 m temperature was used. A cloud of points with much higher PT100

temperatures is due to the instrument failure of the temperature difference measurement. The cloud with very high sonic temperatures and PT100 temperatures below zero is from a period 14.2. to 17.2. 1999, where the sonic anemometer shows unrealistically high values for the temperature. In the same period also the sonic wind speeds are partly suspicious. For this period the sonic temperature measurements are assumed to be erroneous.

For the other measurements a temperature dependent mean shift between the temperatures of the two sensor types and a large scatter around this can be seen. Figure 37 shows the difference between the two temperature sensor types versus the absolute temperature at 10 m. Shown are all measurement records and the bin-averaged (bin width 2ºC) values with the root mean square error of the records with respect to their bin values. A clear dependency on the ambient temperature can be seen.

It is believed that this shift is due to a temperature dependent behaviour of the sonic anemometer. This behaviour is also described by (Mortensen and Højstrup, 1995). It is probably caused by small temperature dependent variations in the properties of the transducers and the electronics. They estimate the maximum temperature dependent error to 5 K for a temperature range of –10º to +30ºC on the basis of measurements in an environmental chamber at zero wind speed. The bin values here show a mean shift of –0.9º to +1.3ºC with a root mean square error of 0.3º to 0.8ºC.

Additionally to the observed temperature dependent shift considerable scatter can be observed in the measurement. The reason for these variations is not known. A systematic dependency on other measured parameters could not be found.

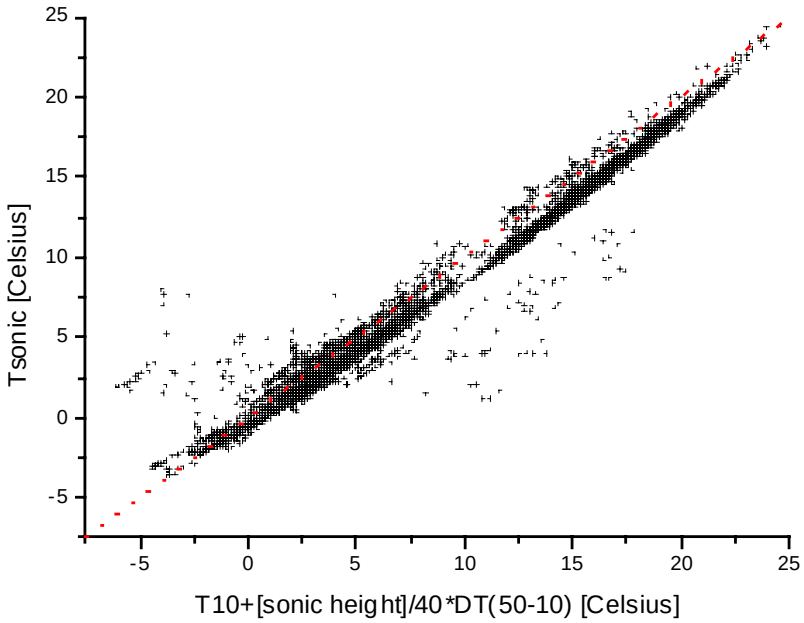

Figure 36: Scatter plot of air temperatures measured by the sonic anemometer and the one measured by the PT100 sensor at 10 m height corrected for height with the temperature difference measurement

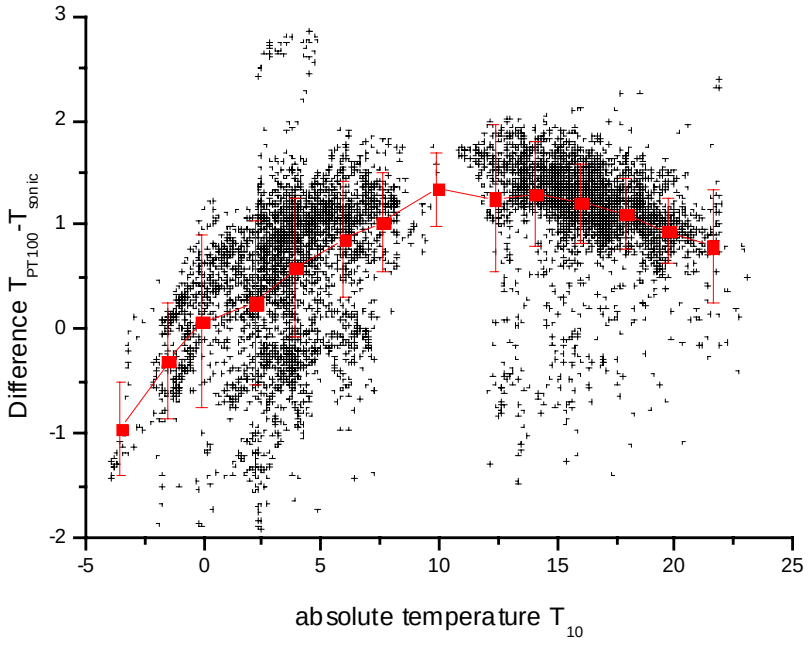

Figure 37: Difference between the two temperature sensor types versus the absolute temperature at 10 m; shown are all measurement records and the bin-averaged (bin width 2ºC) values with the root mean square error of the records with respect to their bin values

Figure 38 shows the temperature difference between air and water versus temperature difference measurement between 10 and 50 m height. For an air temperature difference of about –0.4ºC the atmosphere is neutrally stratified. As expected, the mean temperature difference between water and air is about 0ºC in this case. For stable stratification it is positive, i.e. the air temperature is higher than the water temperature, and for unstable stratification negative.

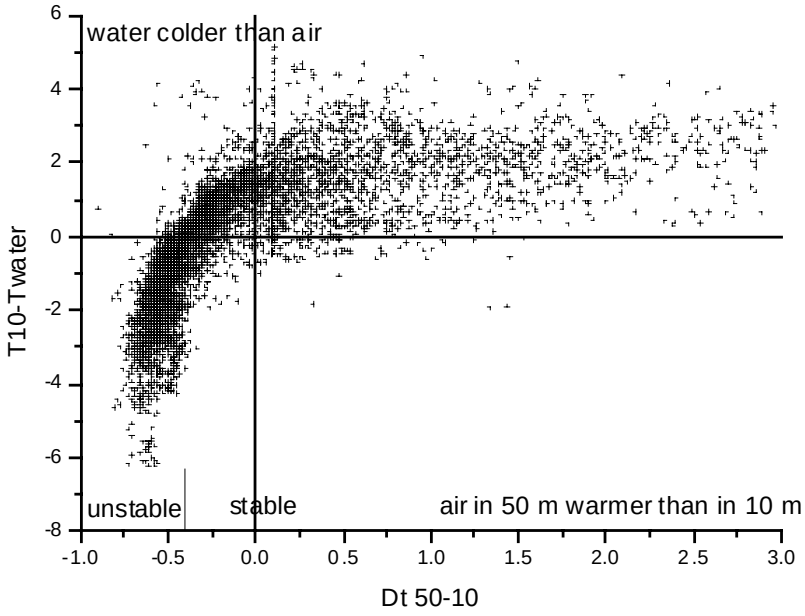

Figure 38: Temperature difference between air and water versus temperature difference measurement between 10 and 50 m height

4.2.12 Heat flux

The heat flux is measured by the sonic anemometer as the co-variance between fluctuations in vertical velocity and temperature. The time series shows considerable scatter especially for very unstable situations, but also sometimes for stable situations. Additionally there are often single values with large deviations, often corresponding to wind speed changes. The frequency distribution is shown in Figure 39.

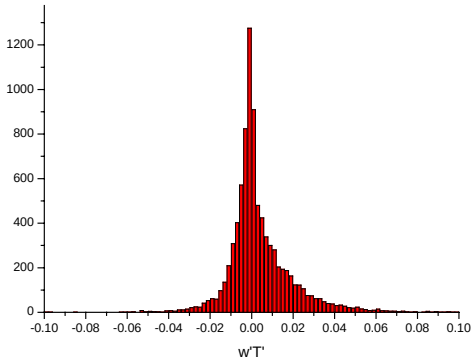

Figure 39: Frequency distribution of the w'T' covariance measurement

The covariance w'T' can be seen as a measure for the atmospheric stability since it describes the heat flux in the atmosphere. It can therefore be compared with the temperature differences between different heights (here 10m and 50m) and the temperature difference between water and air. This is done in Figure 40 and Figure 41.

Problems with the measurement of the w'T' covariance have been described in chapter 4.1.3. A high noise level was found for some records, which gave rise to large uncertainties in the w'T' values. This can be found as very large scatter in Figure 40 and Figure 41.

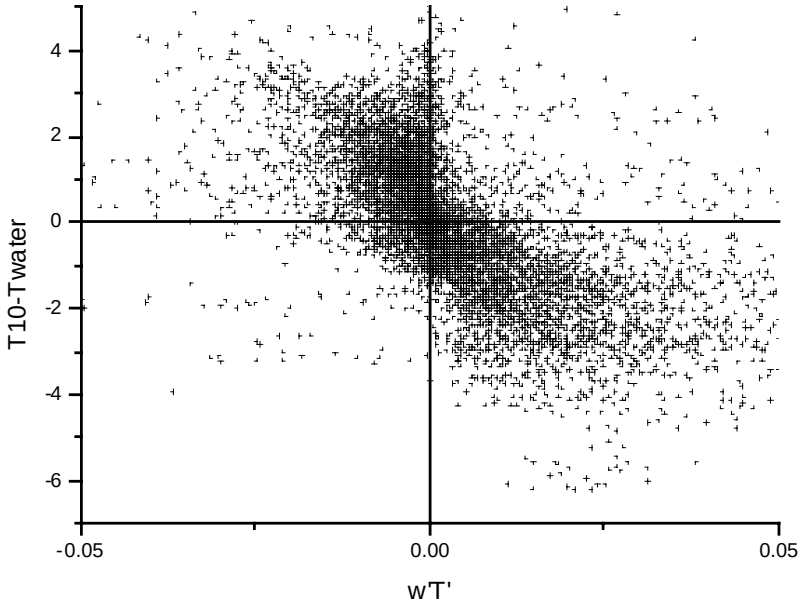

Figure 40: Temperature difference between air and water versus covariance w'T'

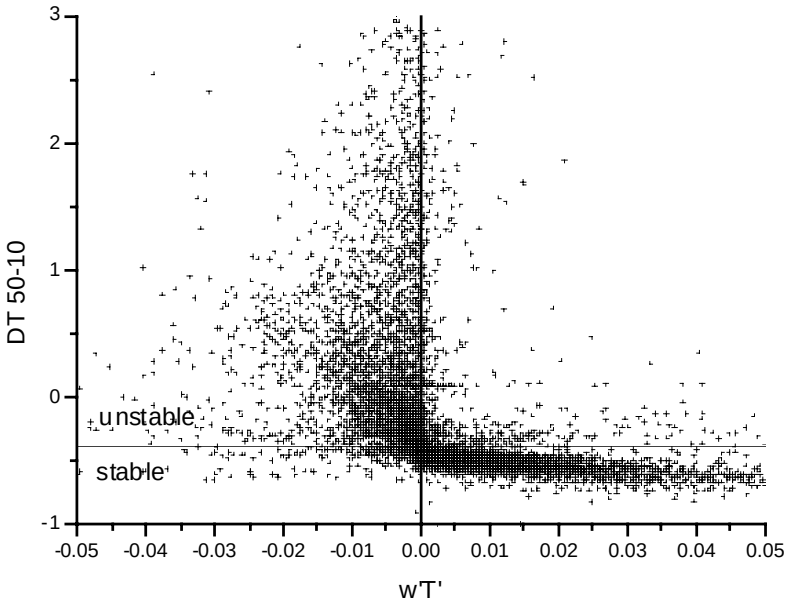

Figure 41: Temperature difference measurement between 10 and 50 m height versus covariance w'T'

4.2.13 Friction velocity

The friction velocity is derived from the co-variances u'w' and v'w' measured by the sonic anemometer with the relation:

$$u_* = \left(\overline{u'w'}^2 + \overline{v'w'}^2\right)^{0.25}$$

The frequency distribution of the co-variances u'w' and v'w' and of the friction velocity are shown in Figure 42. Figure 43 shows a scatter plot of the friction velocity versus wind speed at 50 m height.

The time series plots of the co-variances and friction velocity frequently show single records with large deviations from the surrounding values. These can also be seen as outliners with high u* values in Figure 43. These records can often be identified with large gradients in wind speed and/or direction. To remove these erroneous values the time series has been filtered with a gradient filter similar to the adaptive filter described in chapter 4.1.1. The limit for the gradient between to consecutive records is set to 0.15 m/s + 0.03 m/s * d, where d is the number of records dismissed since the last valid record. This removes most of the spikes as can be seen in Figure 44, where the scatter plot of the friction velocity versus wind speed at 50 m height is repeated after filtering.

However, there are still large variations between consequent records in the measured time series. The reason for these variations is not known.

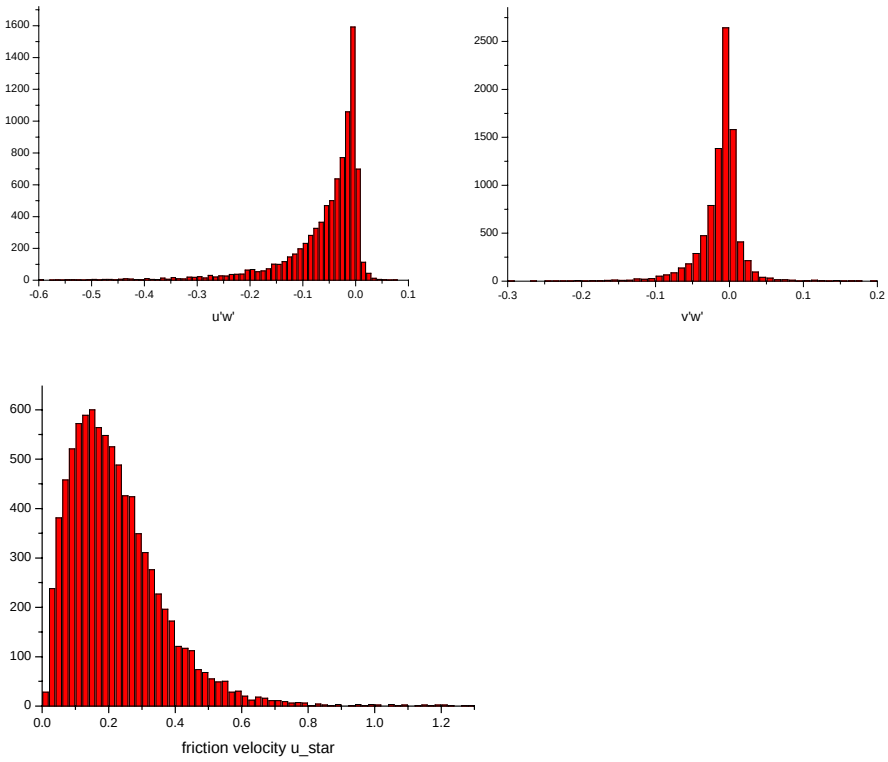

Figure 42: Frequency distributions of the co-variances u'w' and v'w' measured by the sonic anemometer and the friction velocity (m/s) derived from them

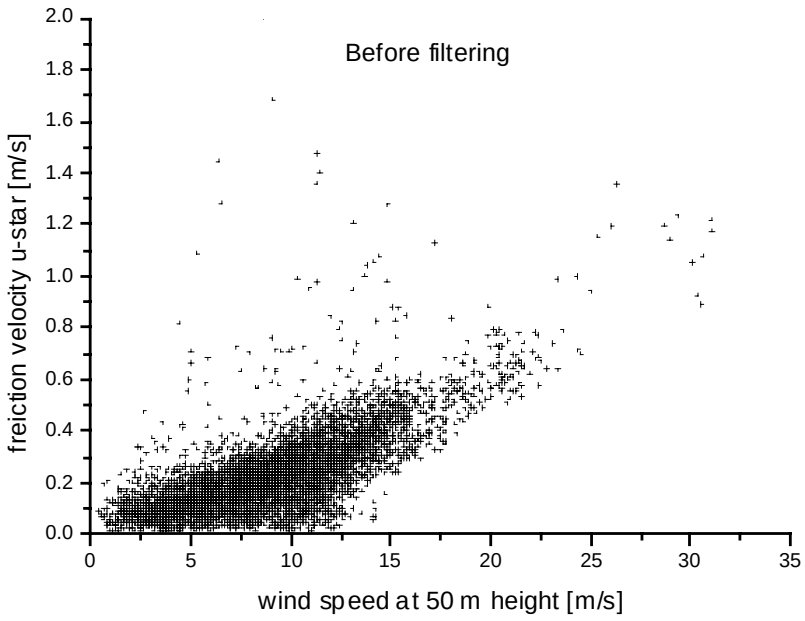

Figure 43: Friction velocity versus wind speed at 50 m height before filtering

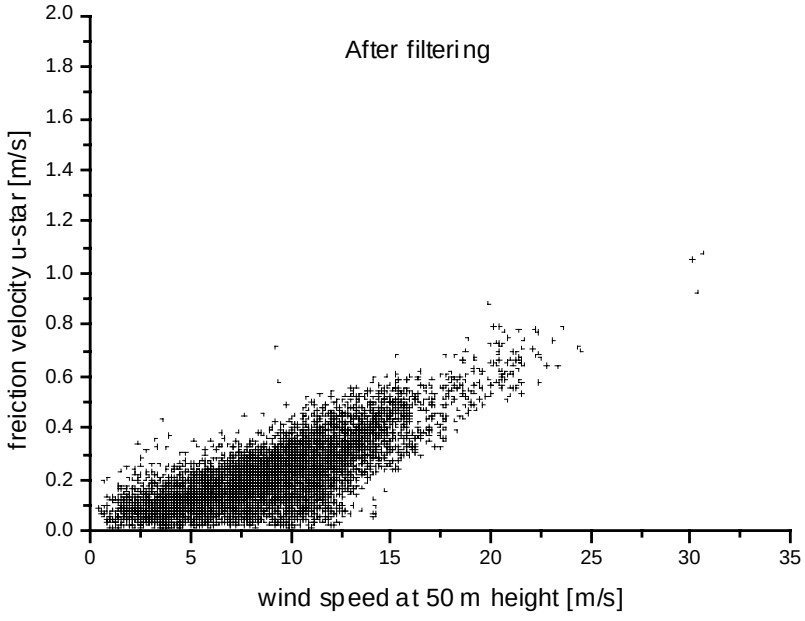

Figure 44: Friction velocity versus wind speed at 50 m height after filtering

5 Data processing and data bases

The measurement data from the field measurement at Rødsand are used for different purposes. Therefore two different data bases have been developed in addition to the data base of stored raw data.

The meteorological data base is a Paradox based data base of all statistical data (30-minute averages for the DAQ-system and 10-minute averages for the Aanderaa system). An automatic quality control procedure is used, which is described in chapter 5.1.

The met-ocean time series is a file in ASCII format with half-hourly averages of meteorological and oceanographic data. It is used for detailed analysis of the interaction between wind, waves and current. For the analysis of the wave data it is necessary to use the measured fast samples time series (see chapter 4.1.1). Therefore only measurement periods were used, where these were available. Time periods where the wave or current sensors were not in operation were also dismissed. Therefore this time series contains less records than the meteorological data base (see chapter 5.3). The data processing, calibration and quality control of this time series are described in chapter 5.2, a file description is given in chapter 5.4.

5.1 Data processing and quality control for meteorological data base

5.1.1 Data processing

The data processing for the meteorological data base is done in the measurement computer at the time of the measurement. The processed measurement records can be collected by remote control of the measurement station and no site visit is necessary. The following processing steps are done:

Cup anemometers and wind vane

1. Calculate mean, standard deviation and extremes of wind speeds and direction

Sonic anemometer

1. Align co-ordinate system to the mean wind direction (u,v,w)-co-ordinate system
2. Calculate mean, standard deviation and extremes of wind speed and direction
3. Remove linear trends in wind speed and direction
4. calculate co-variances
5. calculate u_*

Temperatures and temperature difference

1. Calculate means, standard deviation and extremes

Acoustic wave recorder

1. Calculate means, standard deviation and extremes of water level measurement

Current measurement

1. Calculate means, standard deviation and extremes of x and y component of water current

5.1.2 Conditions for data screening

In addition to the visual inspection of the data, which is conducted when new data are collected, a screening program has been developed to identify data which are possibly erroneous. Each type of data is given a normal or operating range including both mean and standard deviation which is shown in Table 10. In addition the screening program calculates the running mean and identifies deviations from this value. This procedure identifies times when instruments are not functioning. Error codes are stored for application with the data.

Table 10: Criteria for quality control for the meteorological data base

	Mean value	Standard Deviation	Response	Continuity	Ex-tremes
Wind speed	0 to 50 m/s	0 to 2 m/s (or 0.2 × mean)	Mean ≠ RM	Mean within ±50 % of RM	0 to 50 m/s
Wind direc-tion	0 to 360 °	0 to 45°	Mean ≠ RM	Mean within ±30° of RM	0 to 360°
Absolute temperature	-15 to 35°C	0 to 1°C	Mean ≠ RM	Mean within ±5°C of RM	Mean ±5°C
Differential temperature	-2 to 7°C	0 to 1°C	Mean ≠ RM	Mean within ±1°C of RM	Mean ± 2°C
Wave height	3 to 5 m	0.02 to 0.5m	Mean ≠ RM	Mean within ±0.5 m/s of RM	
Current meter	-1 to 1m/s	0 to 0.25m/s			
Current Di-rection	0 to 360°	0.01 to 10°			
Wave status	0.59 to 0.61	0.48 to 0.59			
Current status	0.59 to 0.61	0.48 to 0.59			

5.2 Data processing and quality control for met-ocean time series

5.2.1 Data processing

Data processing for the met-ocean time series is done with the collected fast sampled data. Less data are available for this analysis since it requires site visits to collect these data. Additionally, for this time series only data were processed, where the wave and current instrument were functioning. 14794 data files stored on 8 data CDs have been processed. 8775 records have been found to contain the necessary data (wave and current instrument working). The steps of the data

processing are listed below, followed by the parameters used for calibration and correction.

Data processing steps

Cup anemometers and wind vane

1. Calculate mean, standard deviation and extremes of wind speed and direction
2. Exclude wind speed measurements in mast shade and correct wind speed measurements for boom and mast flow distortion
3. For Aanderaa data the averaging period is changed from 10 min to 30 min, time stamp is changed to DNT and giving the start of an averaging period

Sonic anemometer

1. Filter all 4 sonic signals for spikes
2. Align co-ordinate system to the mean wind direction (u,v,w)-co-ordinate system
3. Calculate mean, standard deviation and extremes of wind speed and direction
4. Remove linear trends in wind speed and direction
5. calculate co-variances
6. Calculate spectra
7. calculate u_*

Temperatures and temperature difference

1. Calculate means, standard deviations and extremes
2. For Aanderaa data the averaging period is changed from 10 min to 30 min, time stamp is changed to DNT and giving the start of an averaging period

Acoustic wave recorder

1. Filter wave signal for spikes
2. Remove linear trend in water level height
3. Calculate wave spectrum
4. Derive integral wave parameters (H_s, T_{50}, BW, T_m, T_z) and mean water level

Current measurement

1. Find and count errors in measurement, when the current sensor reaches its measurement limit
2. Calculate mean current speed and direction from x- and y-components

Data calibration parameters

The calibration offsets for the wind and current direction sensors have been determined in chapter 4.2. For convenience they are listed again in Table 11.

Table 11: Calibration offsets for wind and current direction measurements

Parameter	time period	calibration
WD_30	>19990601	+7°
S_dir	<19990601	+83°
	>19990601	+92°
Cur-dir	all	+Cur-align

Data correction parameters for mast flow distortion

Wind speed measurements of the cup and sonic anemometers (mean and gust values) were corrected for influences of the flow distortion around the measurement mast for all directions except the direct mast shadow, where they were omitted. The method developed in (Højstrup, 1999) has been used with the correction factors shown in Table 12.

Table 12: Correction factors for the mast flow distortion correction with the (Højstrup, 1999) method

Instrument	Ratio for flow from mast to instrument	Ratio for flow from instrument to mast
cup anemometer 10m	1.033	0.994
cup anemometer 30m	1.012	0.998
cup anemometer 50m	1.004	0.999
Sonic anemometer	1.005	0.999

5.2.2 Conditions for data screening

To detect erroneous or missing values all data have been screened with an automatic screening procedure. All conditions for data screening described in chapter 4.2 are summarised in Table 13. Data found erroneous in the data screening procedure were set to the error indicator 999.

Table 13: Conditions for and results of data screening for quality control

Parameter	low limit (incl.)	high limit (incl.)	no. of errors	parameters set to error indicator
WS 50	0	40	854	WS_45, WS_45_stdev, WS_45_max
WS 30	0	40	0	WS_30, WS_30_stdev, WS_30_max
WS 10	0	40	0	WS_10, WS_10_stdev, WS_10_max
$(\text{Cos WD 30})^2$ $+(\text{Sin WD30})^2$	12	-	20	WD_30
WD 30	0	360	0	WD_30
WS Sonic	0	40	0	S_speed, S_dir
WD Sonic	0	360	0	S_speed, S_dir
Wave status	0.58	0.62	14	MSL, Hs, T50, Tm, Tz
Int. duration	1500	2100	0	all (omit record)
WS 50 stdev	0	8	879	WS_45, WS_45_stdev, WS_45_max
WS 30 stdev	0	8	0	WS_30, WS_30_stdev, WS_30_max
WS 10 stdev	0	8	44	WS_10, WS_10_stdev, WS_10_max
WS 45 max	0	60	854	WS_45, WS_45_stdev, WS_45_max
WS 30 max	0	60	0	WS_30, WS_30_stdev, WS_30_max
WS 10 max	0	60	0	WS_10, WS_10_stdev, WS_10_max
MSL	6	9	3	MSL, Hs, T50, Tm, Tz
Hs	0.01	4	8	MSL, Hs, T50, Tm, Tz
T50	1	7	30	T50, Tm, Tz, Hs
BW	0.08	0.25	1326	T50, Tm, Tz
Tm	1	7	24	T50, Tm, Tz, Hs
Tz	1	7	11	T50, Tm, Tz, Hs
Cur-align	0	360	0	Cur-align, Cur-dir
Cur-speed	0	100	0	Cur-speed, Cur-dir
Cur-dir	0	360	1	Cur-speed, Cur-dir
Wave-spikes	0	1500	96	MSL, Hs, T50, Tm, Tz
Cur-err2	0	3	46	Cur-speed, Cur-dir
u-star	gradi-ent	filter	315	u-star

5.3 Availability of the met-ocean time series

Due to different technical problems the availability of the fast-sampled Rødsand measurement is rather low. The data coverage of meteorological data is much better and the availability of the Aanderaa system, which has been employed since May 1999 is nearly 100%.

For wave measurements only time periods with fast sampled data can be used. An overview over times where fast sampled and wind data were available is

given in Figure 45. The days with at least one record available are listed in Table 14. It can be seen that only very few data are available from 1998 (901 records - availability 5%). For 1999 the availability was 42% (7277 records). For January 2000 an availability of 40% is reached (597 records).

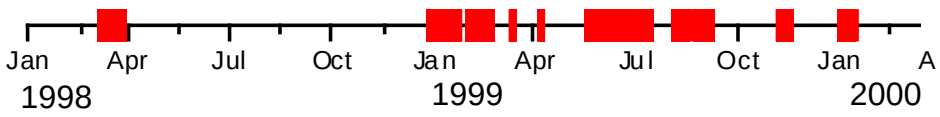

Figure 45: Availability of fast sampled data (including wave and current data)with wind speed and direction for the Rødsand measurement

Table 14: Time periods with at least one data record with fast-sampled data each day

from	to
20.3.98	12.4.98
9.1.99	28.1.99
2.2.99	7.2.99
14.2.99	9.3.99
26.3.99	28.3.99
20.4.99	23.4.99
1.6.99	2.8.99
17.8.99	24.9.99
22.11.99	3.12.99
16.1.00	30.1.00

Because of the short measurement period and the low availability the measured fast-sampled data are not representative of any annual average or climatology. Figure 46 shows the distribution of the available fast-sampled measurement records over the months of the year. Large differences are present with two months with no data and a maximum of about 16% of all data from January. However, despite these large differences both summer and winter data are well represented with 4278 records in the summer (May-October) and 4497 records in the winter.

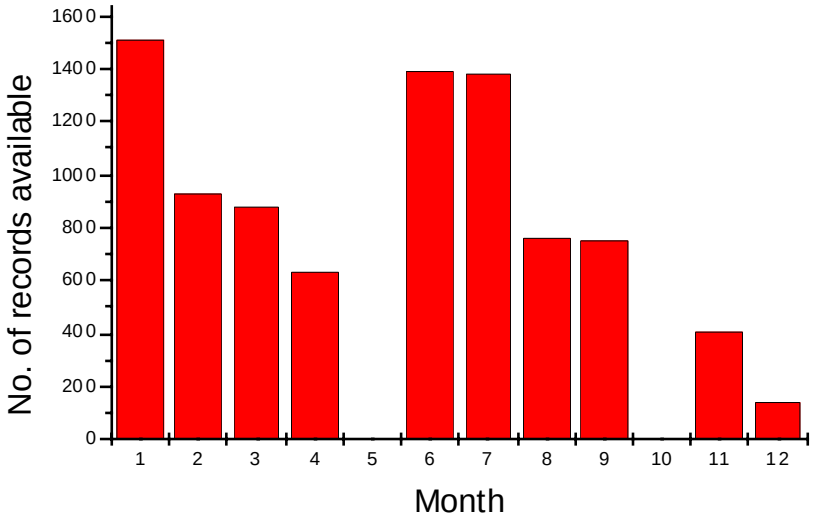

Figure 46: Monthly distribution of available fast-sampled measurement records for wind speed and direction at Rødsand

5.4 File description of the Met-Ocean time series

The data of the measured time series for Rødsand are given in the file METOCEAN.DAT. It consists of 8775 rows with 28 columns. The file specification is given in Table 15. Data are 30 minute averages every 30 minutes. The error indicator is 999 for all parameters.

Table 15: Specifications for Rødsand measurement data file METOCEAN.DAT

Col. no.	Parameter	Measurement unit	Description
1	Name	-	Date and time in format YYY-YMMDDhhmm
2	WS 50	m/s	Mean wind speed from cup anemometer at 50.3 m height*
3	WS 30	m/s	Mean wind speed from cup anemometer at 29.8 m height*
4	WS 10	m/s	Mean wind speed from cup anemometer at 10.2m height*
5	WD 30	degrees clockwise from north	Mean wind direction from wind vane at 29.8m (before 1.6.99) / 27.8m (after 1.6.99)*
6	WS Sonic	m/s	Mean wind speed from sonic anemometer at 46.6m (before 1.6.99) / 42.3m (after 1.6.99)*
7	WD Sonic	degrees clockwise from north	Mean wind direction from sonic anemometer at 46.6m (before 1.6.99) / 42.3m (after 1.6.99)*
8	WS 50 stdev	m/s	Standard deviation of wind speed from cup anemometer at 50.3 m height*
9	WS 30 stdev	m/s	Standard deviation of wind speed from cup anemometer at 29.8 m height*
10	WS 10 stdev	m/s	Standard deviation of wind speed from cup anemometer at 10.2 m height*
11	WS 45 max	m/s	Gust wind speed from cup anemometer at 50.3 m height*
12	WS 30 max	m/s	Gust wind speed from cup anemometer at 29.8 m height*
13	WS 10 max	m/s	Gust wind speed from cup anemometer at 10.2 m height*
14	MSL	m	Mean sea level from AWR
15	Hs	m	Significant wave height from AWR
16	T50	s	Wave period at 50% variance from wave spectrum from AWR
17	Tm	s	Mean wave period from wave spectrum from AWR
18	Tz	s	Mean wave period based on zero crossing frequency from wave spectrum from AWR
19	Cur-speed	cm/s	Water current speed
20	Cur-dir	degrees clockwise from north	Water current direction – direction the water is flowing *towards* (opposite to wind direction definition)
21	T air 10	ºC	Air temperature from Pt 100 sensor at 10.0 m height*
22	T air Sonic	ºC	Air temperature from sonic anemometer at 46.6m (before 1.6.99) / 42.3m (after 1.6.99)*
23	T water	ºC	Sea temperature from Pt 100 sensor
24	DT 50-10	ºC	Air temperature difference from Pt 500 sensors at 10.0 and 49.8 m height*

25	<w'T'>	K m/s	Covariance of vertical wind speed and air temperature fluctuations
26	<u'w'>	m^2/s^2	Covariance of horizontal wind speed in mean wind direction and vertical wind speed fluctuations
27	<v'w'>	m^2/s^2	Covariance of horizontal wind speed perpendicular to the mean wind direction and vertical wind speed fluctuations
28	u-star	m/s	friction velocity, calculated as (<u'w'>^{2}+<v'w'>^{2})^0.25

* instrument heights are given above a mean sea level of 7.7m.

Acknowledgement

The original instrumentation and maintenance of the Rødsand measurement station were funded by the EU-JOULE program and the Danish Energy Ministry's UVE program 'Offshore Wind Resources'. Subsequent instrumentation, operation and maintenance were funded by SEAS Distribution A.m.b.A. Also most of the analysis work on which this report is based was funded by SEAS Distribution A.m.b.A.

Gunnar Jensen (Risø) is responsible for the data compilation from the Aanderaa system at Rødsand and for the Tystofte station. Peter Sanderhoff (Risø) performs data compilation from the DAQ system at Rødsand. The technical support team at Risø, particularly Ole Frost Hansen, and the team at MetSupport are acknowledged for their contribution to the data collection. Mr Kobbernagel of Sydfalster-El performed the maintenance and data collection at Rødsand.

References

Barthelmie, R. J., M. S. Courtney, B. Lange, M. Nielsen, A. M. Sempreviva, J. Svenson, F. Olsen and T.Christensen: Offshore wind resources at Danish measurement sites. Internal report Risø-I-1339(EN). Risø National Laboratory, DK-4000 Roskilde, Denmark. 1998

Barthelmie, R. J., B. Lange and M. Nielsen: Wind resources at Rødsand and Omø Stålgrunde. Internal Report Risø-I-1456. Risø National Laboratory, DK-4000 Roskilde, Denmark. 1999

Deutsches Hydrographisches Institut (ed.): Ostsee-Handbuch. IV.Teil. Zwölfte Auflage, Hamburg 1978; pp.612

Dietrich, G., K. Kalle, W. Krauss and G. Siedler: Allgemeine Meereskunde. Eine Einführung in die Ozeanographie. 3., neubearbeitete Auflage. Berlin, Stuttgart 1975; pp.593

Højstrup, J.: A statistical data screening procedure. in: Meas. Sci. Technol. vol.4, 1993; pp.153-157

Højstrup, J.: Vertical extrapolation of offshore wind profiles. in: Proceedings of the 1999 European Wind Energy Conference, Nice, France; 1999

Højstrup, J., B. Lange, R. J. Barthelmie, A. M. J. Pedersen, F. A. Olsen and J. Svenson: Offshore wind resources at selected Danish sites. Internal report Risø-I-1156(EN). Risø National Laboratory, DK-4000 Roskilde, Denmark. 1997

Lange, B.: Data analysis of the Rødsand field measurement. Part I: Report, Part II: Time series plots of Rødsand measurement data. Internal report Risø-I-1631(EN). Risø National Laboratory, DK-4000 Roskilde, Denmark. 2000

Mortensen, N. G. and J. Højstrup: The solent sonic - response and associated errors. Proceedings of the 9th symposium on meteorological observations and instrumentation, March 27-31, 1995, Charlotte, N.C., 1995

Bibliographic Data Sheet **Risø-R-1268(EN)**

Title and authors

Description of the Rødsand field measurement

Bernhard Lange, Rebecca Barthelmie and Jørgen Højstrup

ISBN	ISSN
87-550-2885-3(Internet)	0106-2840

Department or group	Date
Department of Wind Energy	May 2001

Groups own reg. number(s)	Project/contract No(s)

Pages	Tables	Illustrations	References
59	15	46	11

Abstract (max. 2000 characters)

The meteorological and oceanographic field measurement Rødsand has been established 1997 at the site of the planned offshore wind farm Rødsand, 12 km south of Lolland. Its primary aim is to provide data about the environmental conditions needed in the planning process of the wind farm. Additionally, the field measurement provided a valuable data set for scientific research. This report provides a documentation of the Rødsand field measurement, including the site, the measurement station itself, the extensive quality control of the data and the data processing.

Descriptors INIS/EDB

COASTAL WATERS; DATA ANALYSIS; DATA PROCESSING; DENMARK; MEASURING INSTRUMENTS; METEOROLOGY; OCEANOGRPAHY; OFFSHORE SITES; QUALITY CONTROL; SITE CHARACTERIZATION; WATER WAVES; WIND;